NASA TN D-1034

TECHNICAL NOTE

D-1034

LARGE-SCALE WIND-TUNNEL TESTS OF AN AIRPLANE MODEL WITH AN UNSWEPT, TILT WING OF ASPECT RATIO 5.5, AND WITH FOUR PROPELLERS AND BLOWING FLAPS

By James A. Weiberg and Curt A. Holzhauser

Ames Research Center
Moffett Field, Calif.

NATIONAL AERONAUTICS AND SPACE ADMINISTRATION

WASHINGTON

June 1961

NATIONAL AERONAUTICS AND SPACE ADMINISTRATION

TECHNICAL NOTE D-1034

LARGE-SCALE WIND-TUNNEL TESTS OF AN AIRPLANE MODEL WITH AN UNSWEPT, TILT WING OF ASPECT RATIO 5.5, AND WITH FOUR PROPELLERS AND BLOWING FLAPS

By James A. Weiberg and Curt A. Holzhauser

SUMMARY

Tests were made of a large-scale tilt-wing deflected-slipstream VTOL airplane with blowing-type BLC trailing-edge flaps. The model was tested with flap deflections of 0° without BLC, 50° with and without BLC, and 80° with BLC for wing-tilt angles of 0°, 30°, and 50°. Included are results of tests of the model equipped with a leading-edge flap and the results of tests of the model in the presence of a ground plane.

INTRODUCTION

To investigate the effectiveness of BLC trailing-edge flaps on a tilt-wing propeller-driven transport, tests were made of the model of reference 1 modified so that the wing could be tilted with respect to the fuselage. The aerodynamic characteristics of the model with a leading-edge flap and the effects of the presence of a ground plane are also presented. The data are presented without analysis.

NOTATION

b	wing span, ft
c	wing chord parallel to plane of symmetry, ft
$\bar{c}$	mean aerodynamic chord, $\frac{2}{S}\int_0^{b/2} c^2 dy$, ft
C_D	drag coefficient including thrust, $\frac{\text{measured drag}}{q_\infty S}$
C_L	lift coefficient, $\frac{\text{lift}}{q_\infty S}$
C_{L_α}	slope of lift curve, per deg

$C_{L_{max}}$ maximum lift coefficient

C_m pitching-moment coefficient, $\frac{\text{pitching moment}^1}{q_\infty S \bar{c}}$

C_μ jet momentum coefficient, $\frac{w_j}{g q_\infty S} V_j$

D propeller diameter, ft

F resultant force, lb

g acceleration of gravity, 32.2 ft/sec^2

h height of $\frac{\bar{c}}{4}$ above ground plane ($\alpha = 0^\circ$), ft

i_t angle of stabilizer relative to fuselage reference line, deg

J propeller advance ratio, $\frac{V_\infty}{nD}$

L lift, lb

n propeller angular velocity, rps

p free-stream static pressure, lb/sq ft

p_d' total pressure in flap duct, lb/sq ft

q_∞ free-stream dynamic pressure, lb/sq ft

R gas constant for air, 1715 ft^2/sec^2 $^\circ$R

S wing area, sq ft

T thrust, lb

T_d duct temperature, $^\circ$R

T_c' thrust coefficient, $\frac{T}{q_\infty S}$

V_j jet velocity assuming isentropic expansion, $\sqrt{\frac{2\gamma}{\gamma - 1} RT_d \left[1 - \left(\frac{p_\infty}{p_d'}\right)^{\frac{\gamma-1}{\gamma}}\right]}$, fps

V_∞ free-stream velocity, fps

w_j weight rate of air flow through nozzle, lb/sec

y spanwise distance, perpendicular to plane of symmetry, ft

[1]Moments are presented about the center shown in figure 2(c).

A524

α angle of attack of fuselage reference line, deg

δ_f flap deflection measured in plane normal to hinge line, deg

δ_w wing tilt measured from a wing-down position having 8.3° incidence of the root chord with respect to the fuselage reference line, deg

γ ratio of specific heats, 1.4 for air

θ turning angle, $\sin^{-1}\frac{L}{F}$

MODEL

The model shown in figure 1 was used for the tests reported in reference 1 but for the present tests was modified to incorporate wing tilt. The wing could be tilted 30° and 50° from a wing-down position at which incidence of the root-chord was 8.3° with respect to the fuselage reference line. The wing span was shortened by removing the outboard 40 percent of the wing span. The geometry of the model tested is shown in figure 2(a) and pertinent dimensions are given in table I.

The blowing boundary-layer control system on the flaps is described in reference 2. Details of the jet nozzle are shown in figure 2(b). The height of the jet nozzle was 0.060 inch.

The model was equipped with 4 three-bladed propellers. The geometric characteristics of these propellers are given in reference 1. The blade angle at 0.75 blade radius was 21.5°. The propellers were rotated in a clockwise direction, viewed from the rear.

The full-span leading-edge flap used on the model for some of the tests is shown in figure 2(b). The contour of the flap was the same as the leading edge of the wing.

TESTS AND CORRECTIONS

Tests were made at free-stream velocities from 0 to 93 fps ($q_\infty = 10$, a Reynolds number of 2.8 million based on the wing mean aerodynamic chord of 5.18 feet). The data presented in the figures include the direct propeller forces as well as the aerodynamic forces. The propeller thrust characteristics are given in figure 3. This relationship between T_c' and J was assumed invariant with thrust-axis inclination.

Moments are presented about the center shown in figure 2(c).

For some tests the model was mounted in the presence of a ground plane. The location of this ground plane in relation to the model is shown in figure 2(a). For these ground plane tests, corrections to the lift, drag, and pitching moment were made for the tare due to the struts. Tunnel wall corrections were not applied to any of the data.

RESULTS

The basic lift, drag, and pitching-moment characteristics of the model are presented in figures 4 to 6.[2] Data are presented for flap angles of 0°, 50°, and 80°, and wing-tilt angles of 0°, 30°, and 50°. Lift data are summarized in figures 7(a) to 7(c). Presented as functions of thrust coefficient are lift coefficient at constant angle of attack (6° and -24°), $C_{L_{max}}$, and lift curve slope, C_{L_α}. A 5 2 4

The primary effect of wing tilt was to reduce the fuselage angle of attack for a given lift coefficient as can be seen by examining figures 7(b) and 8. Wing tilt was roughly equivalent to an angle-of-attack change.

Above a thrust coefficient of 4, $C_{L_{max}}$ is proportional to T_c' (fig. 7(a)). Tuft observations showed that maximum lift was generally limited by air-flow separation from the wing center section which was unprotected by the propeller slipstream. This flow separation was accompanied by buffeting of the model. The effect of a full-span leading-edge flap (fig. 9) on the wing tilted 30° was an increase in $C_{L_{max}}$ with no increase in the angle of attack for $C_{L_{max}}$.

Drag values presented in figures 4 to 6 include thrust so that $C_D = 0$ corresponds to level unaccelerated flight. Negative values of drag (thrust) correspond to climb, and positive drag corresponds to descent. The lift coefficient for $C_D = 0$ is near $C_{L_{max}}$. Thus, in a descent during a transition (i.e., positive values of drag), the wing would be stalled. Reference 3 has shown that the wing stall in the transition speed range can have a large adverse effect on handling characteristics. The addition of a leading-edge flap to the model (fig. 9) did not increase the drag at maximum lift and, hence, would provide little increase in the glide path angle, based on the values at $C_{L_{max}}$. More effective leading-edge control would require the use of a slat or boundary-layer control.

The aerodynamic characteristics of the model in the presence of a ground plane are shown in figures 10[3] and 11. At the heights tested

---

[2]Because of the difficulty in maintaining constant thrust coefficient at values of 9 and above, the data obtained were crossplotted against thrust coefficient to obtain the curves shown in figures 4 to 6 for constant thrust coefficient and hence are presented without data points.

[3]Data points are omitted from figure 10 for clarity.

($h/\bar{c}$ = 1.8 minimum) the presence of the ground reduced maximum lift coefficient with little or no effect on the slipstream-turning effectiveness or thrust recovery.

Ames Research Center
National Aeronautics and Space Administration
Moffett Field, Calif., April 20, 1961

REFERENCES

1. Weiberg, James A., and Page, V. Robert: Large-Scale Wind-Tunnel Tests of an Airplane Model With an Unswept, Aspect-Ratio-10 Wing, Four Propellers, and Blowing Flaps. NASA TN D-25, 1959.

2. Griffin, Roy N., Jr., Holzhauser, Curt A., and Weiberg, James A.: Large-Scale Wind-Tunnel Tests of an Airplane Model With an Unswept, Aspect-Ratio-10 Wing, Two Propellers, and Blowing Flaps. NASA MEMO 12-3-58A, 1958.

3. Reeder, John P.: Handling Qualities Experience With Several VTOL Research Aircraft. NASA TN D-735, 1961.

TABLE I.- GENERAL GEOMETRIC DIMENSIONS OF THE MODEL

Dimension	Wing	Horizontal surface	Vertical surface
Area, sq ft	145.0	56.5	30.6
Span, ft	28.33	16.03	7.19
$\bar{c}$, ft	5.18	3.50	4.68
Aspect ratio	5.54	4.55	1.69
Taper ratio	0.69	0.45	0.55
Geometric twist, deg	2.2 (washout)	0	0
Dihedral from reference plane, deg	0.8	0	---
Incidence from reference plane, deg	8.3	---	---
Section profile(constant)	NACA 23017	NACA 0012	NACA 0012
Root chord, ft	6.07	4.61	5.88
Tip chord, ft	4.18	2.54	2.65
Sweep of leading edge, deg	2	12	24
Tail length, ft	---	18.03[a]	---

[a]Distance from 0.25 $\bar{c}$ of wing to 0.25 $\bar{c}$ of horizontal tail; 0° wing tilt.

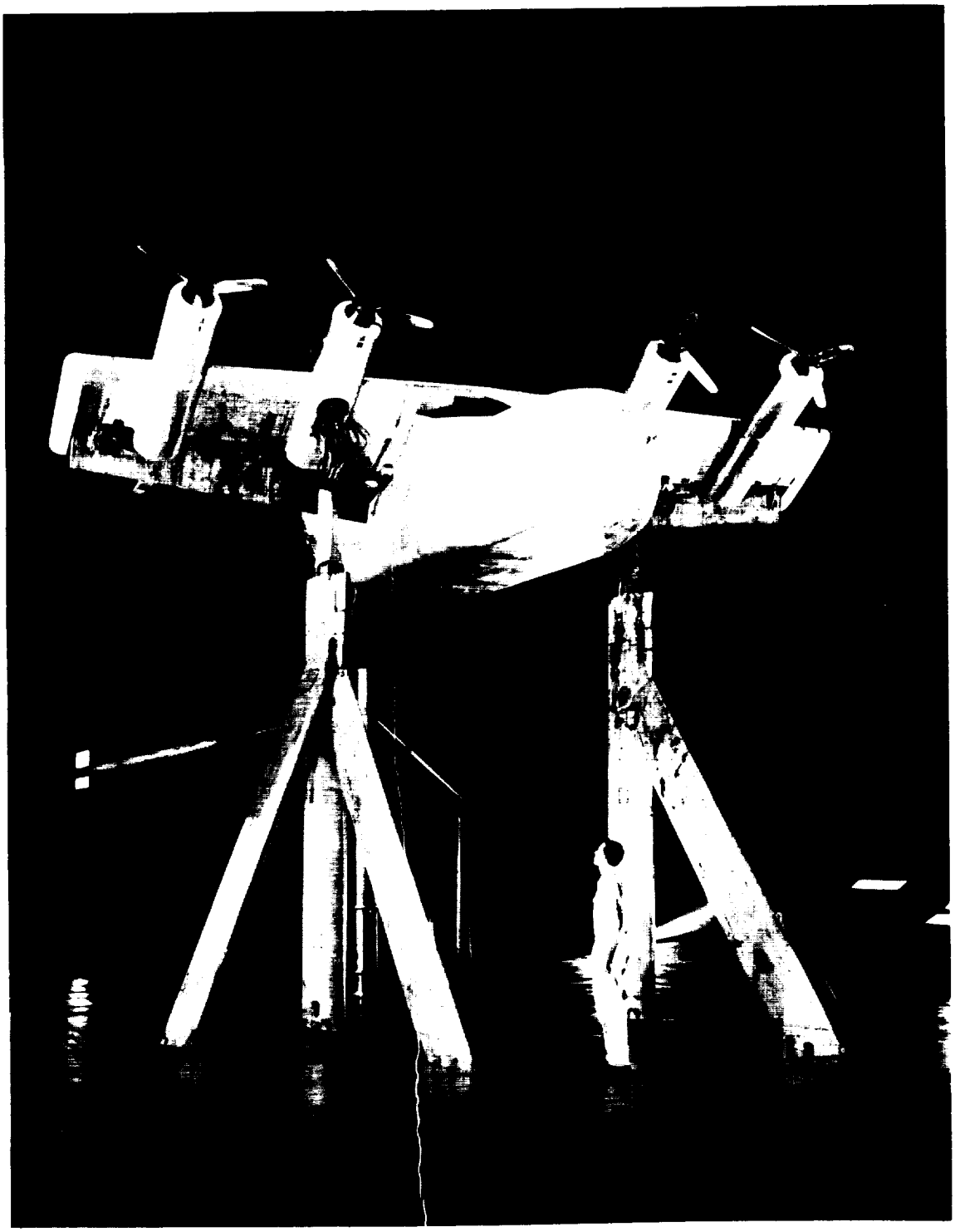

A-25998

Figure 1.- The model mounted in the wind tunnel; $\delta_f = 50^\circ$, $\delta_w = 30^\circ$.

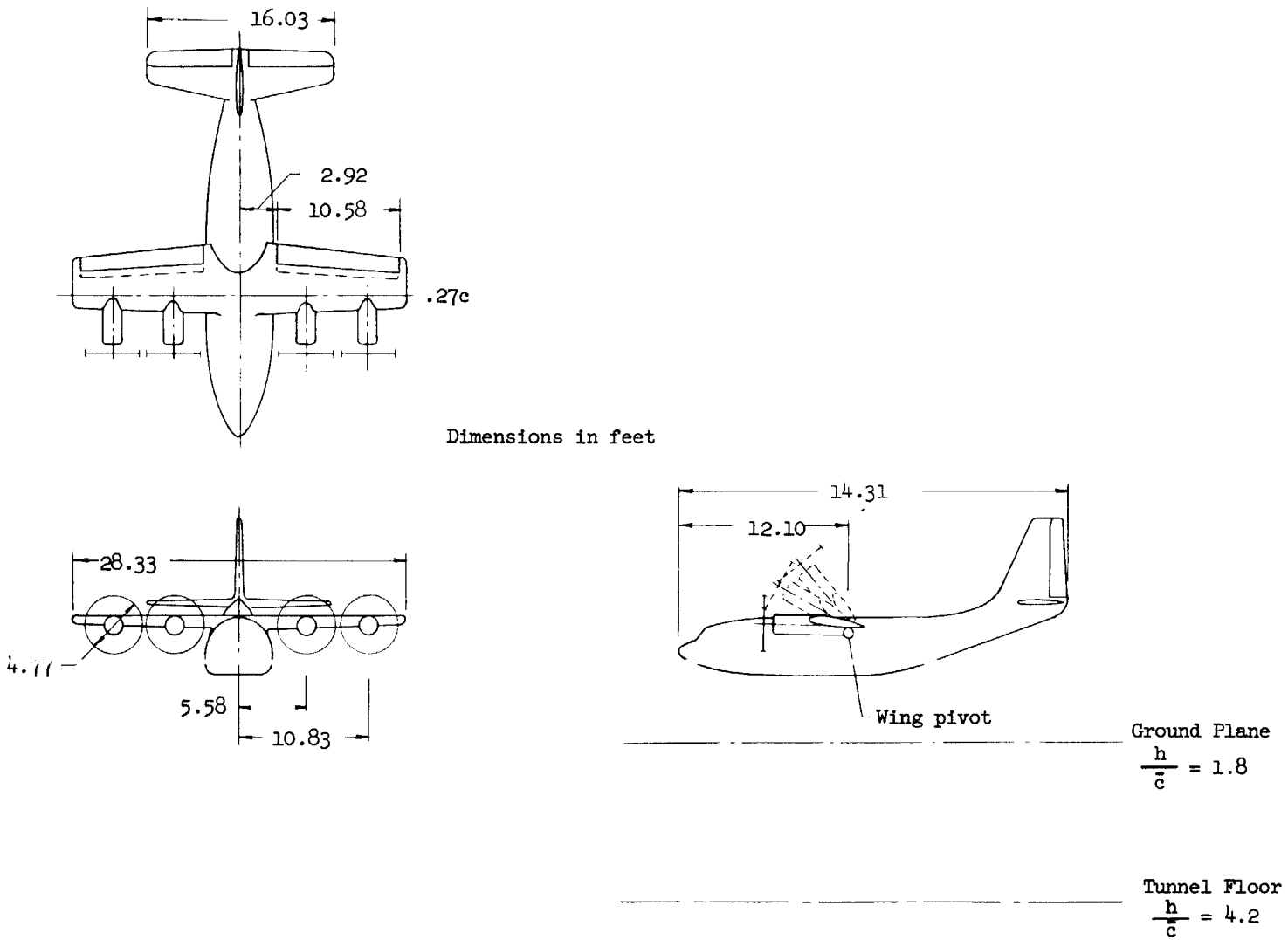

(a) General dimensions.

Figure 2.- Geometry of the model.

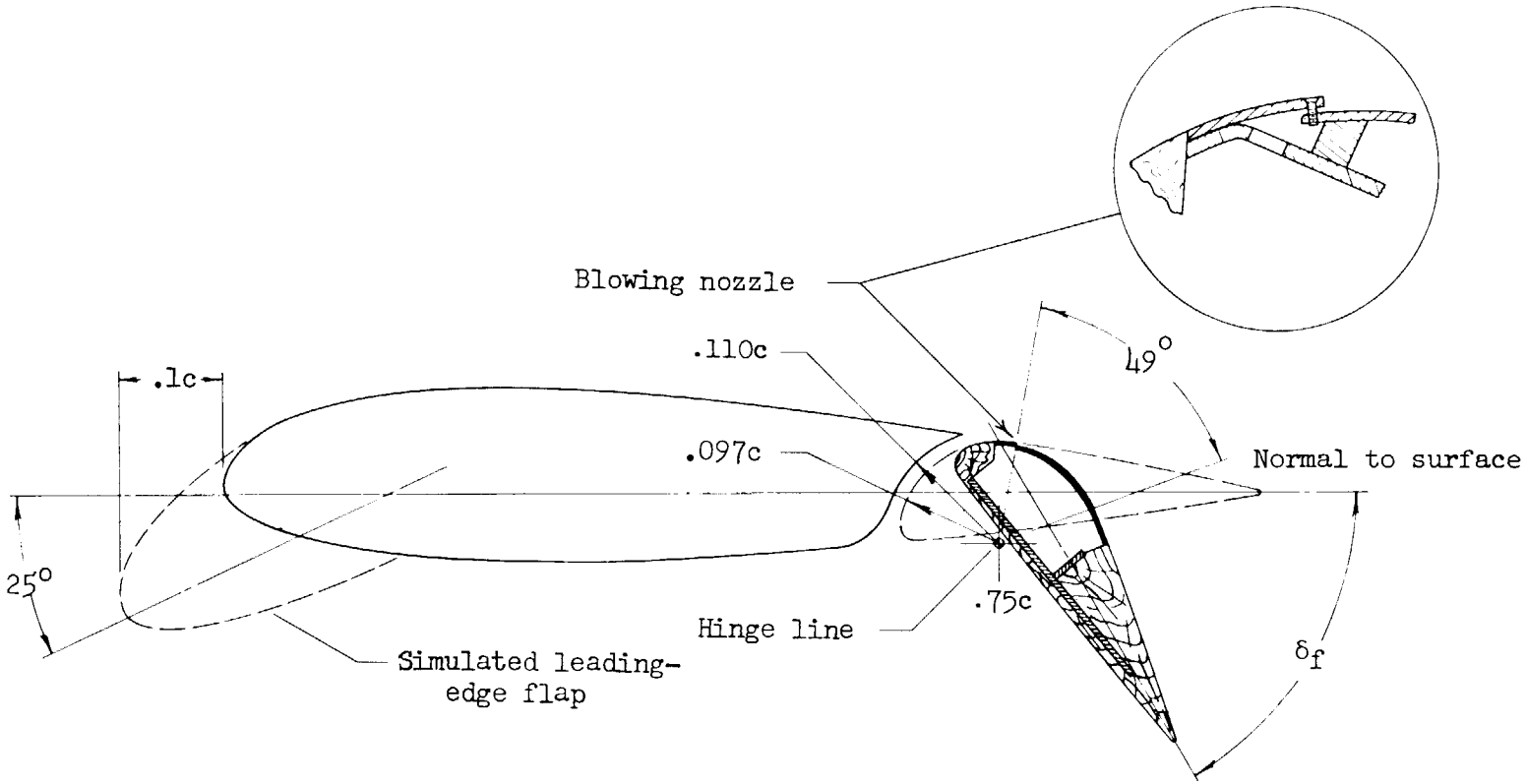

(b) Details of flaps.

Figure 2.- Continued.

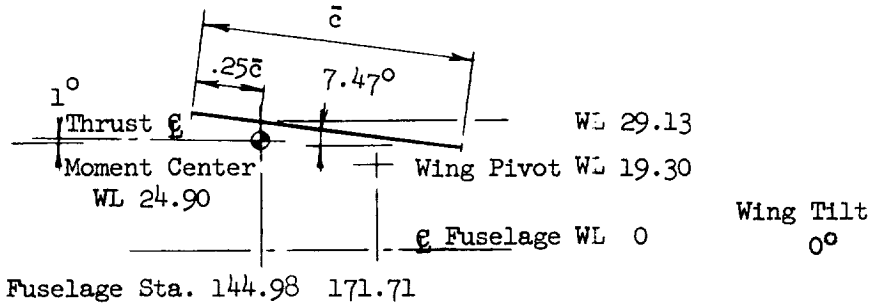

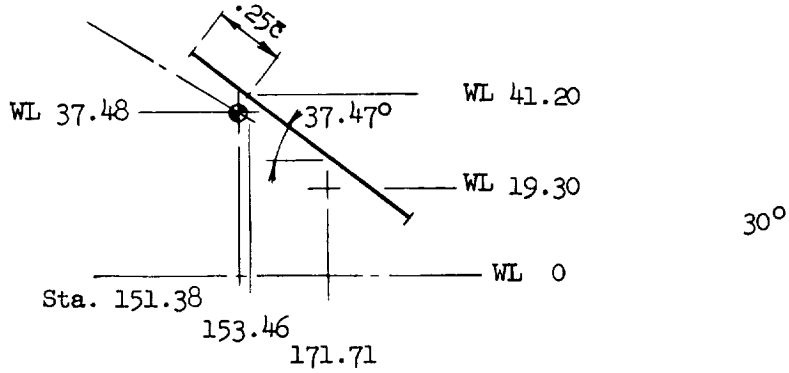

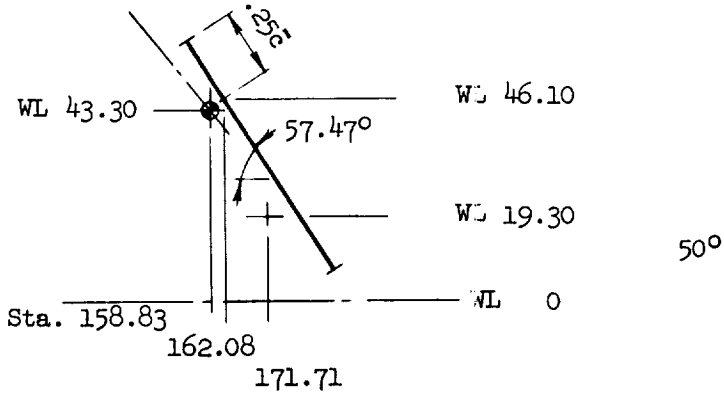

(c) Moment center location.

Figure 2.- Concluded.

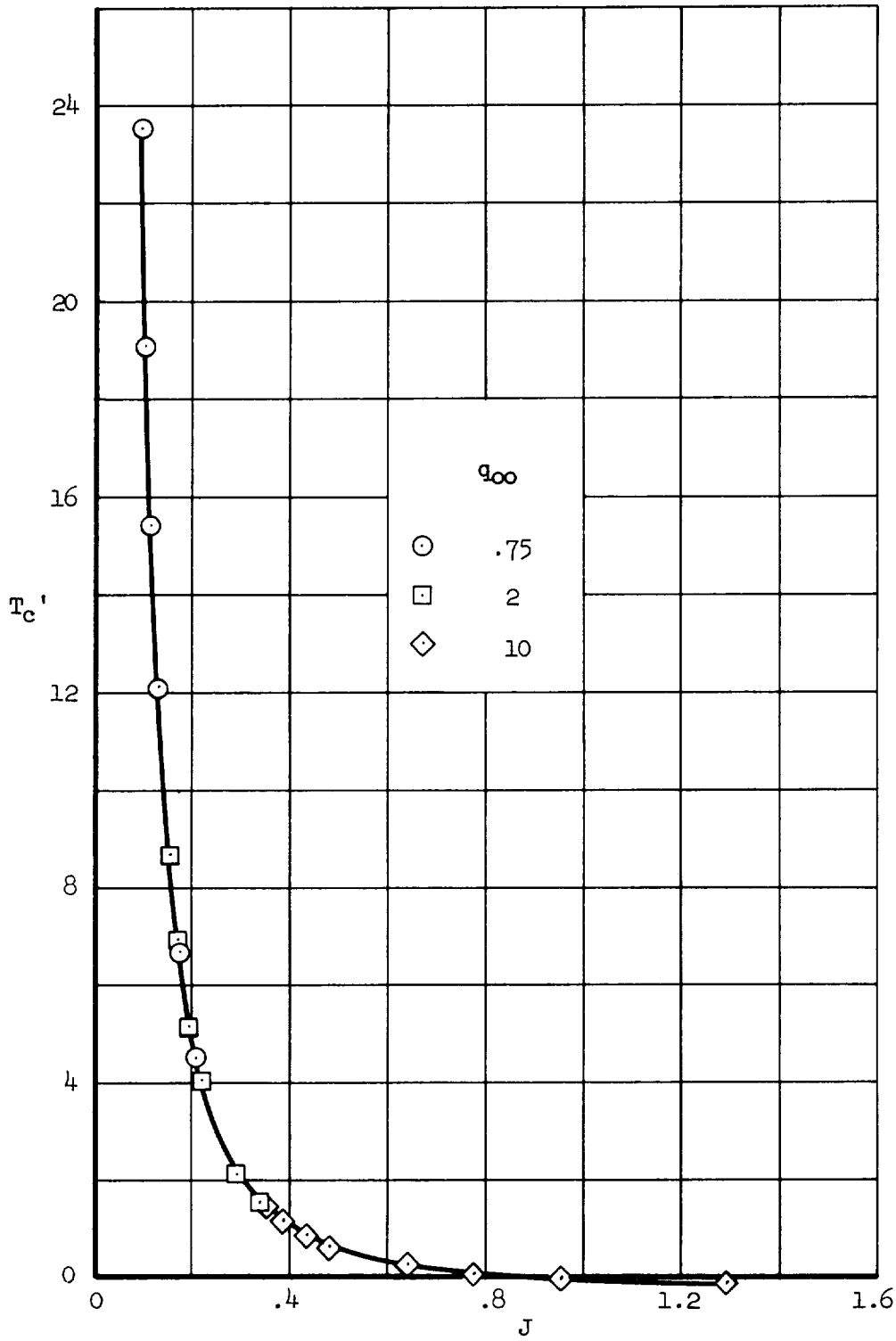

Figure 3.- Propeller thrust characteristics.

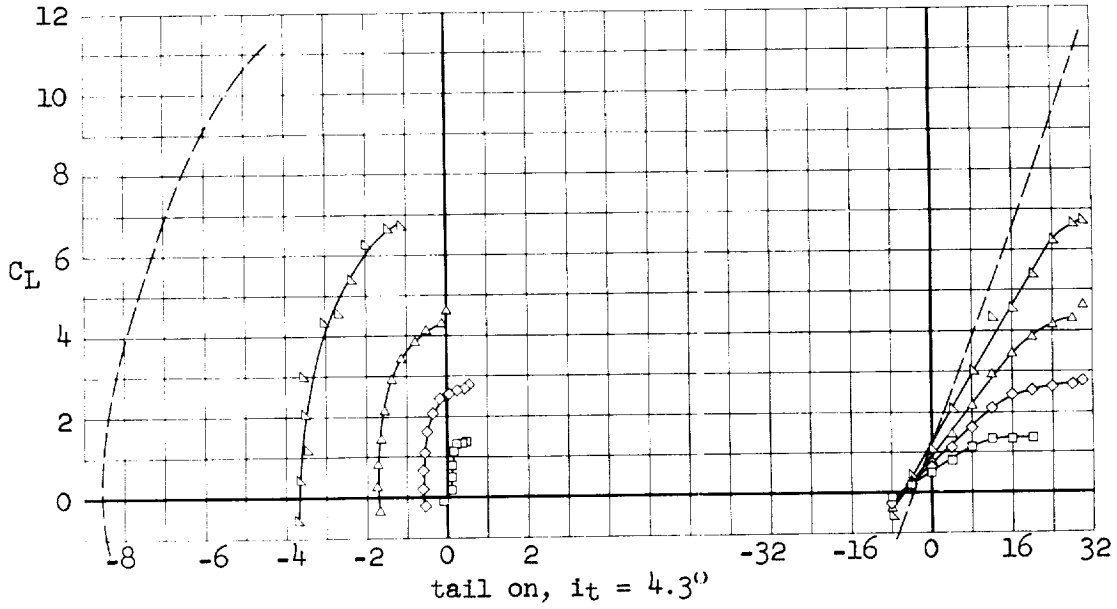

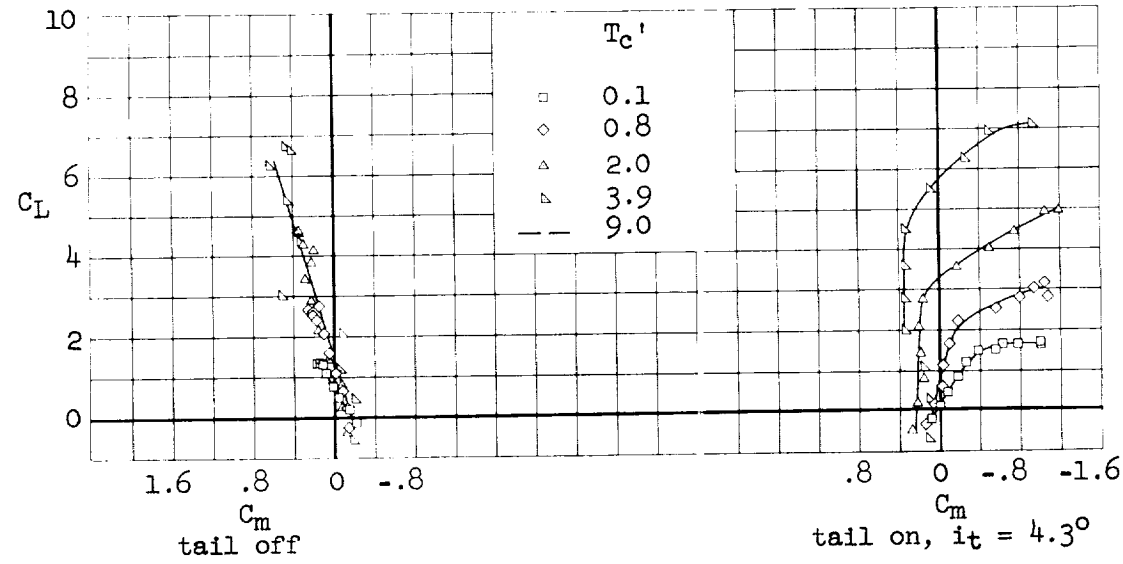

(a) $\delta_f = 0^\circ$, C_μ =)

Figure 4.- Aerodynamic characteristics of the model with 0° wing tilt.

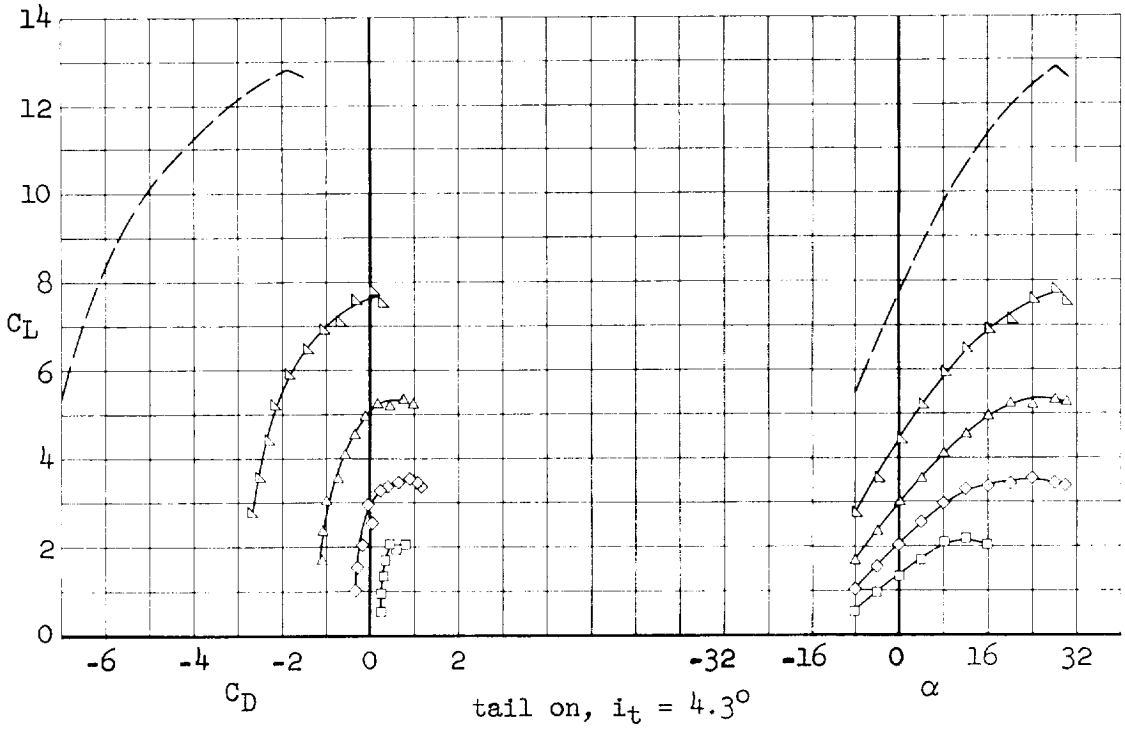

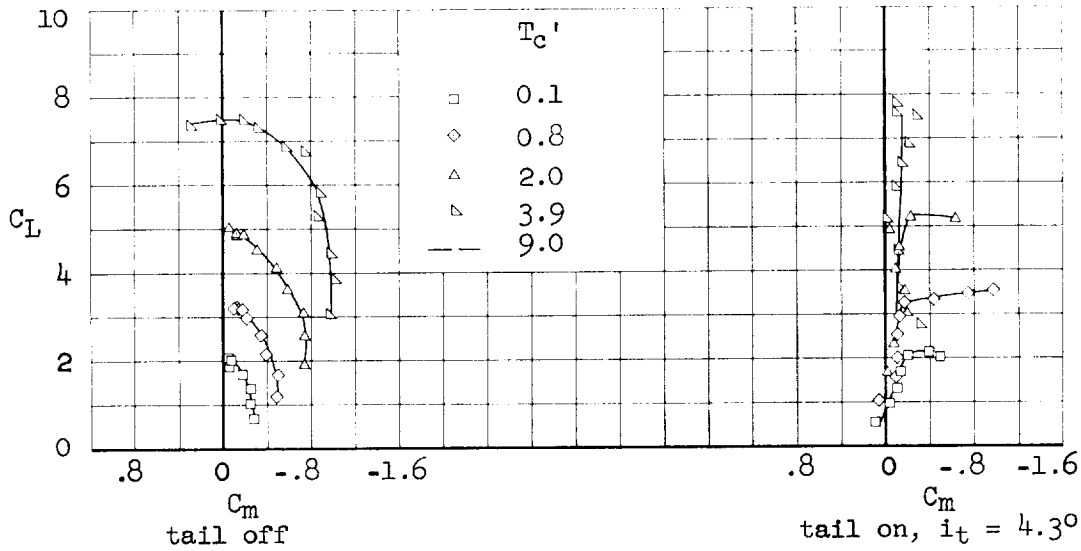

(b) $\delta_f = 50°$, $C_\mu = 0$

Figure 4.- Continued.

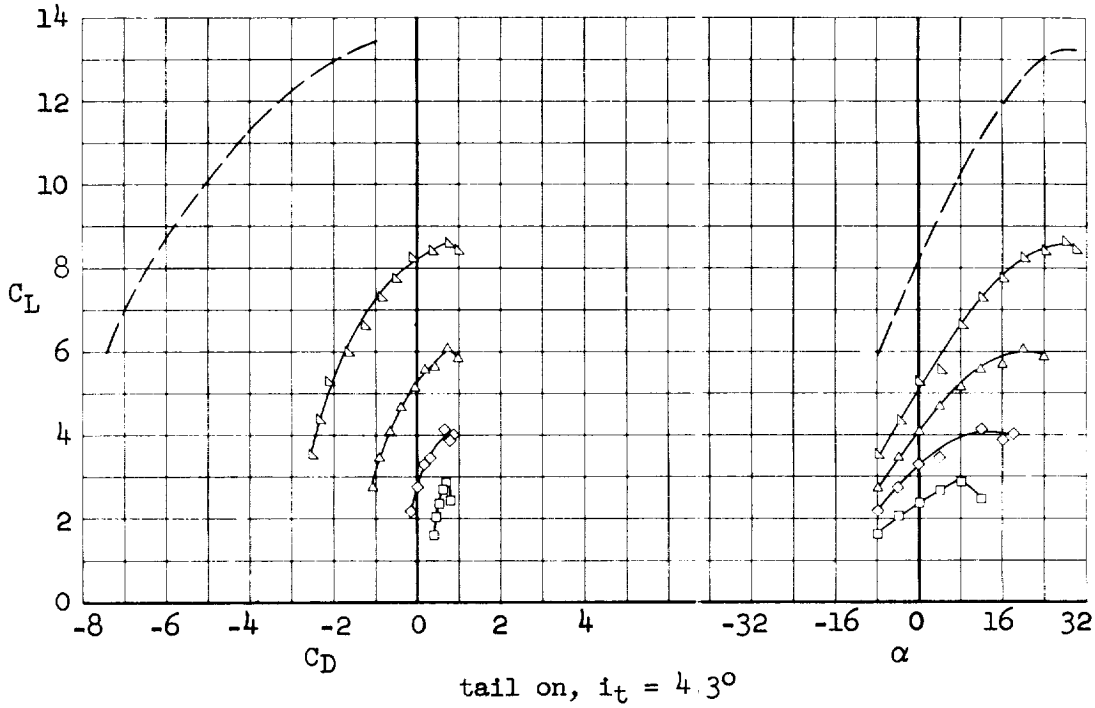

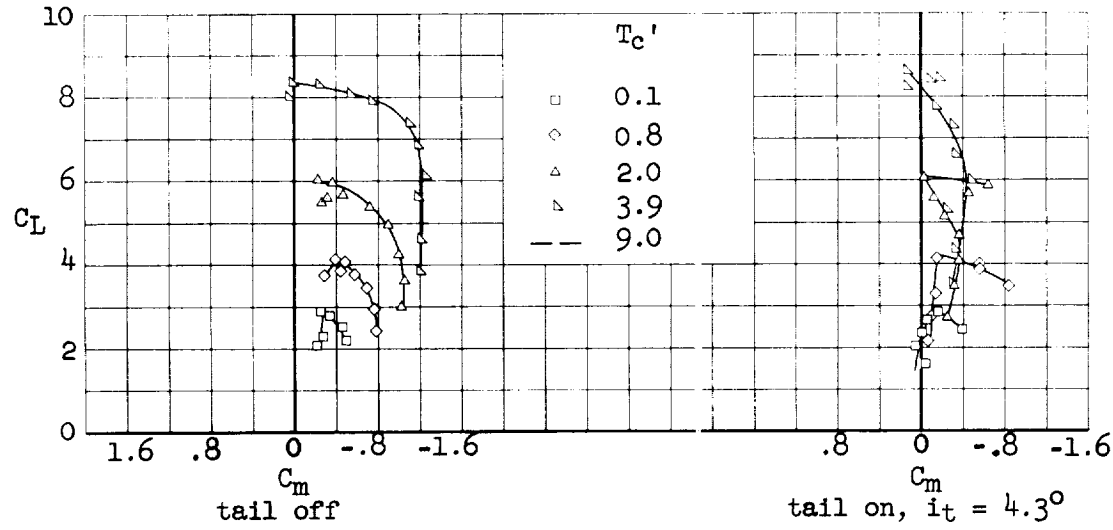

(c) δ_f = 50°, C_μ = 0.065

Figure 4.- Continued.

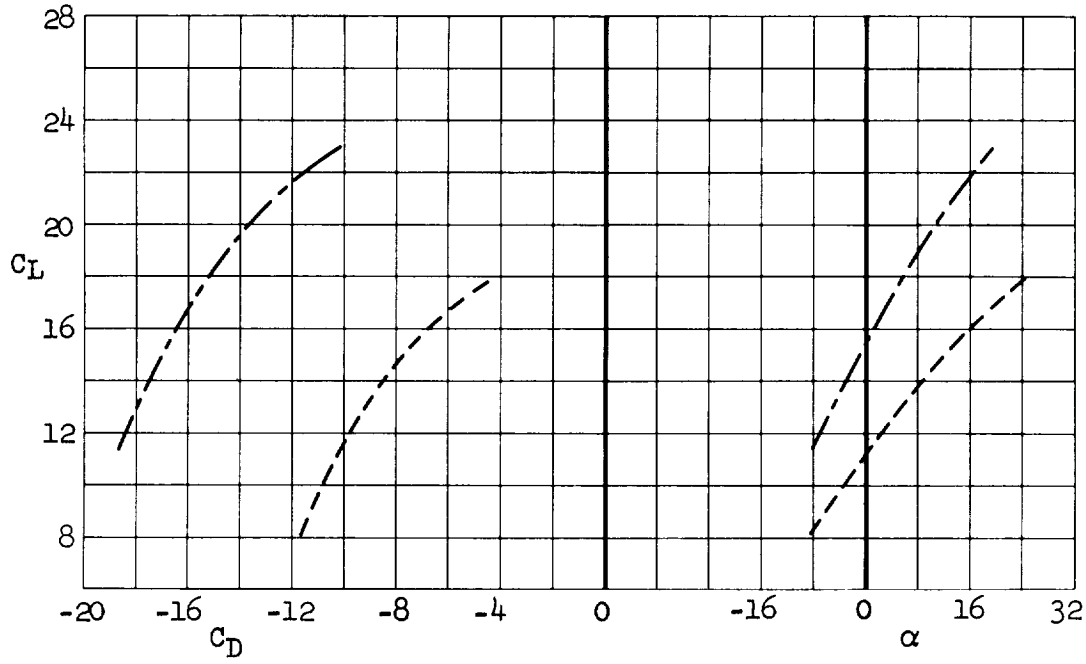

(d) $\delta_f = 50°$, $C_\mu = 0.065$, $i_t = 4.3°$

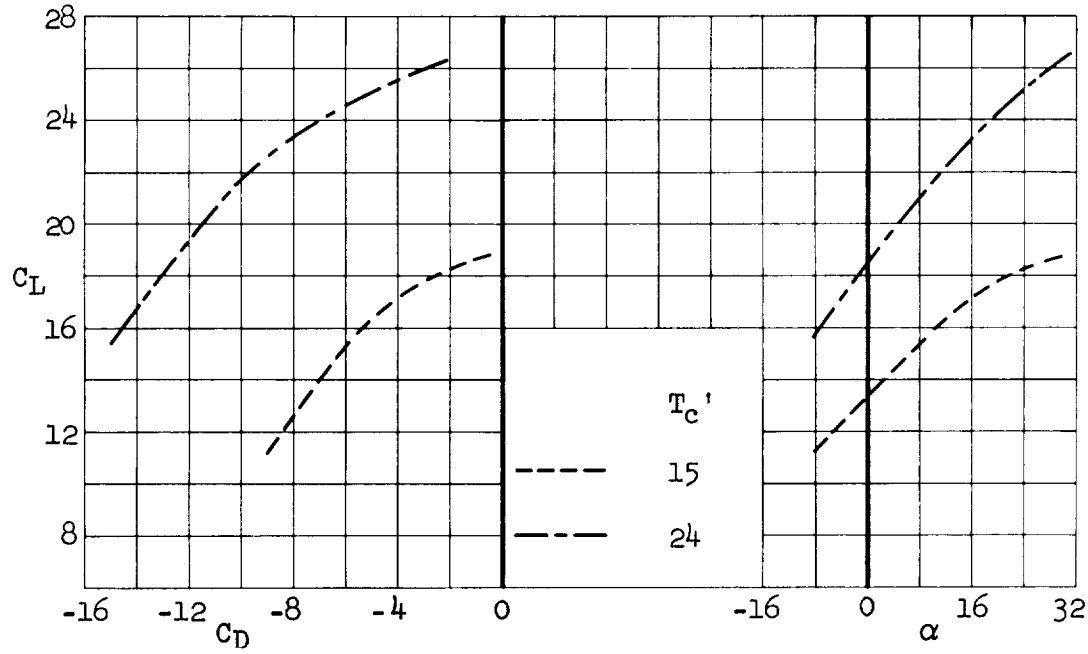

(e) $\delta_f = 80°$, $C_\mu = 0.092$, $i_t = 4.3°$

Figure 4.- Continued.

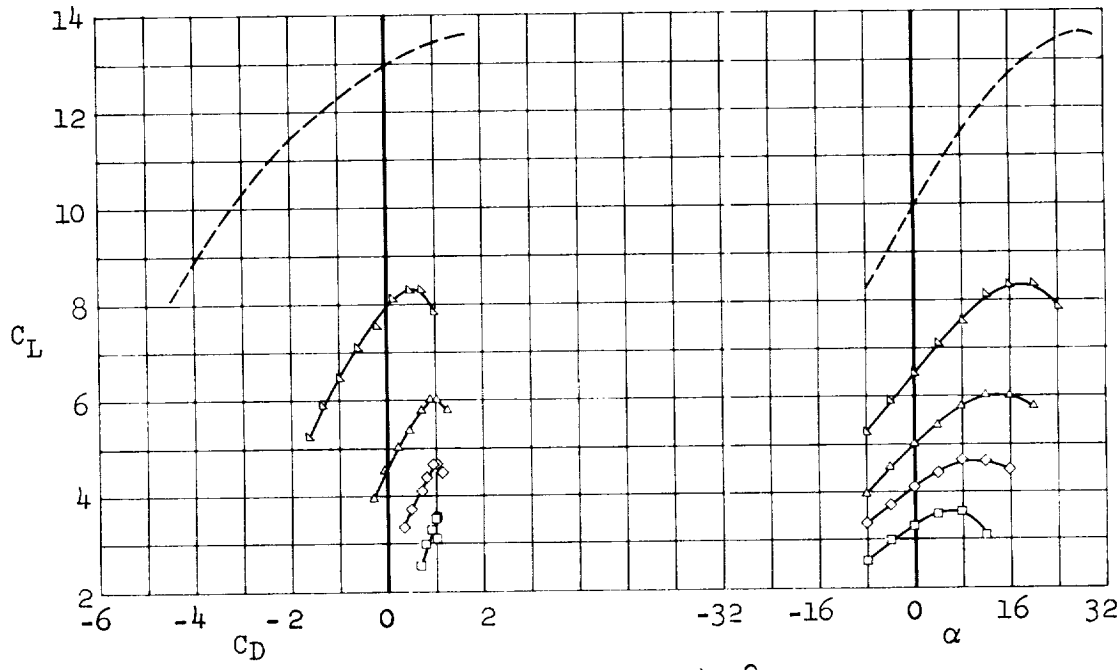

tail on, $i_t = 4.3°$

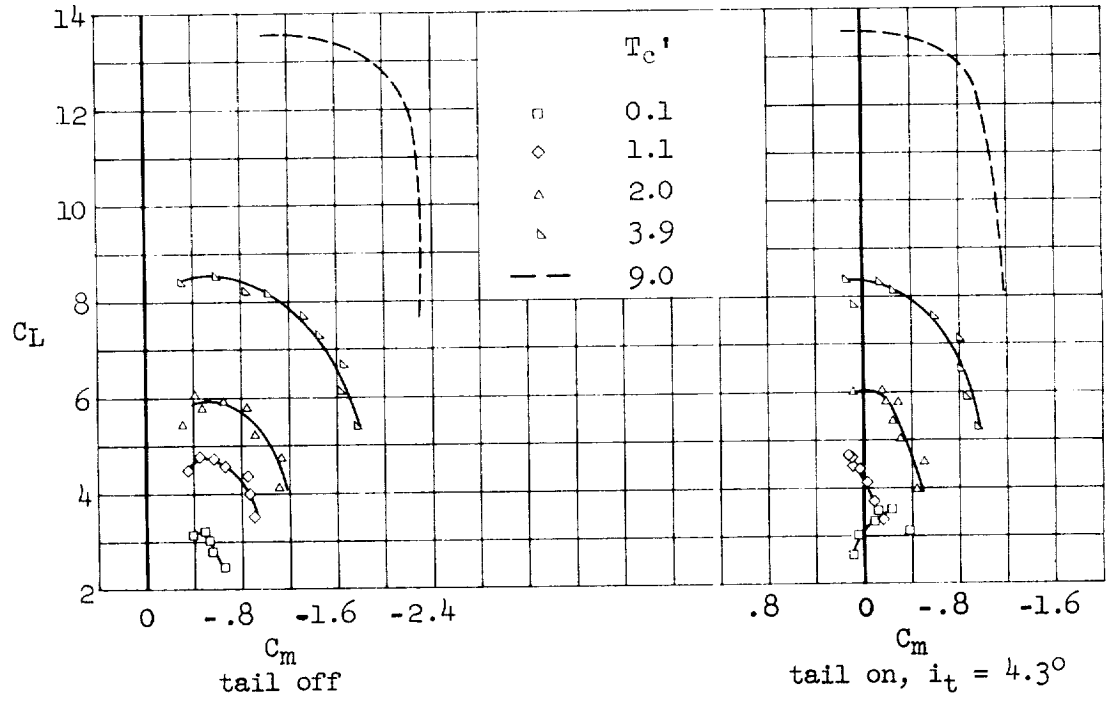

(f) $\delta_f = 80°$, $C_\mu = 0.092$

Figure 4.- Concluded.

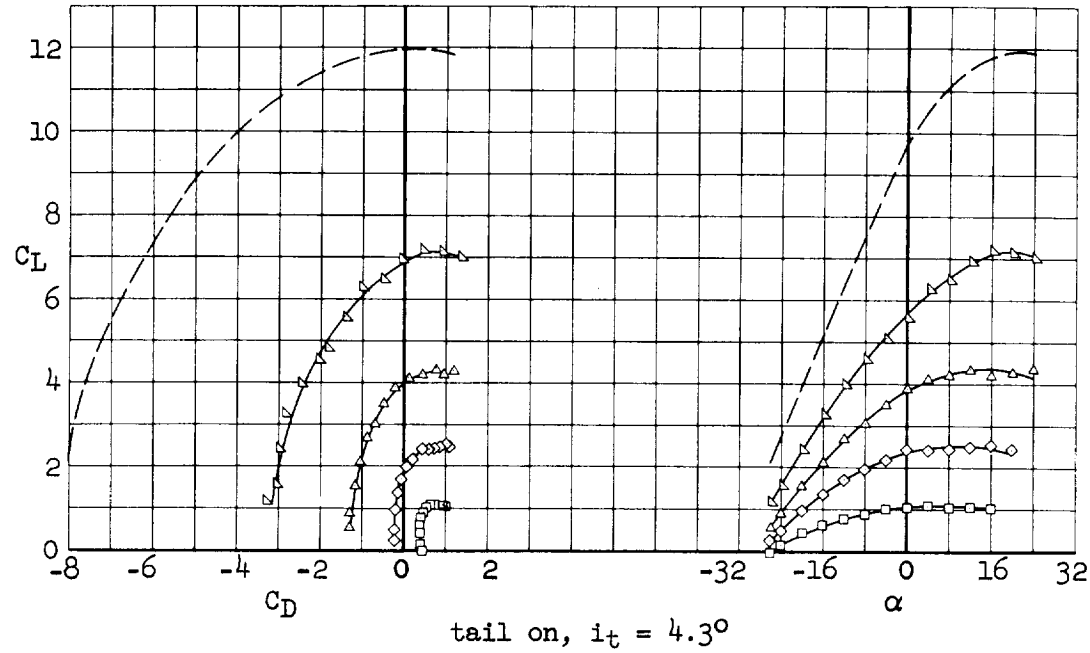

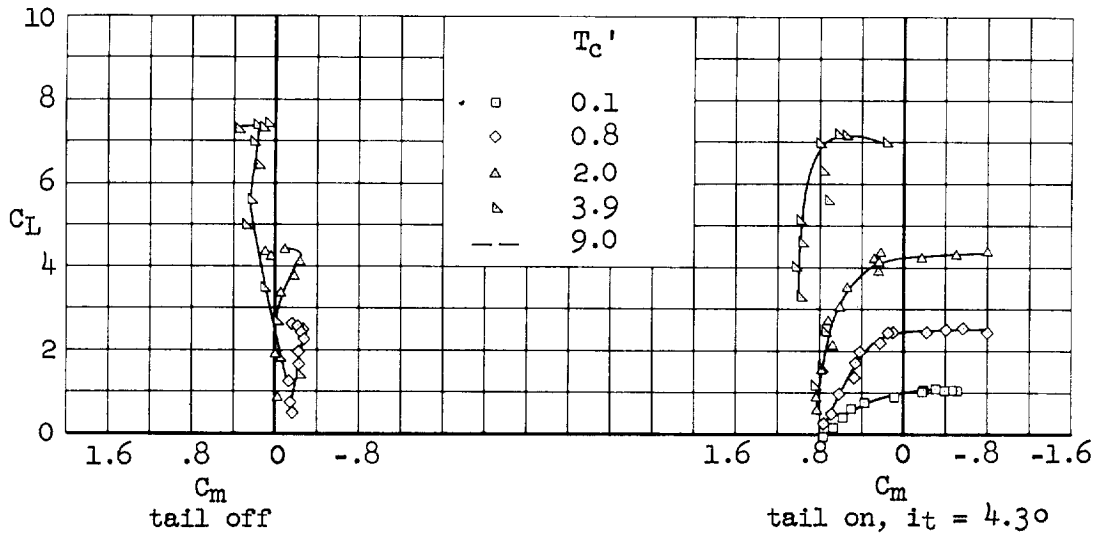

(a) $\delta_f = 0°$, $C_\mu = 0$

Figure 5.- Aerodynamic characteristics of the model with 30° wing tilt.

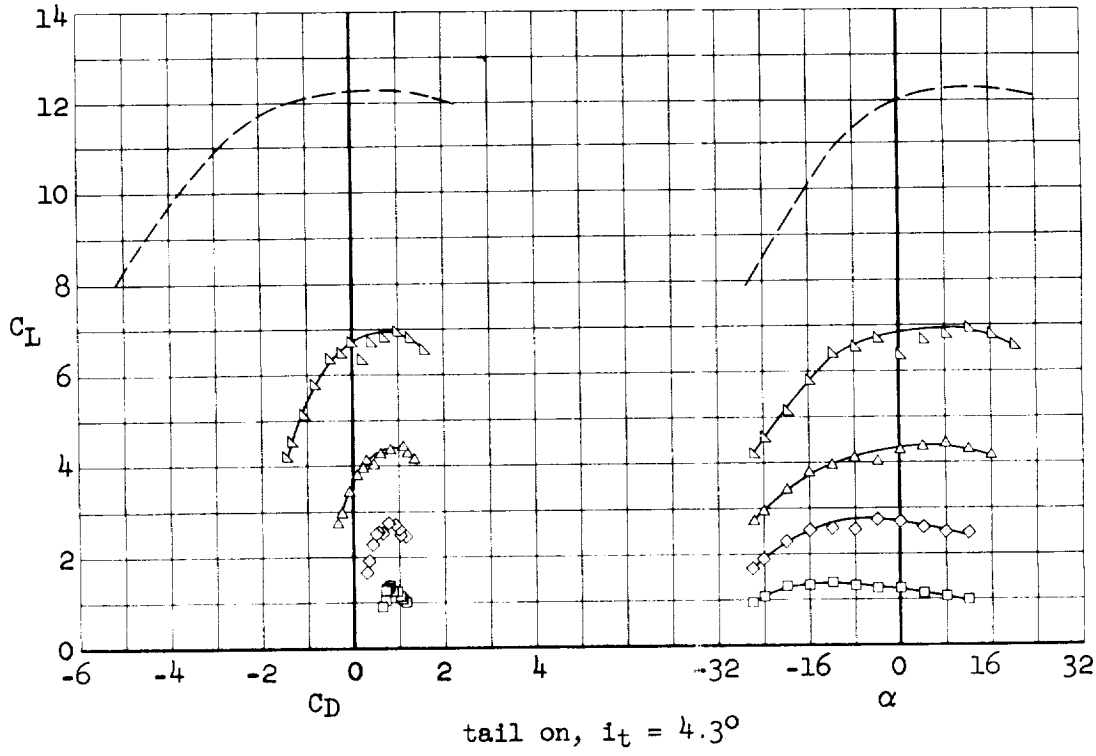

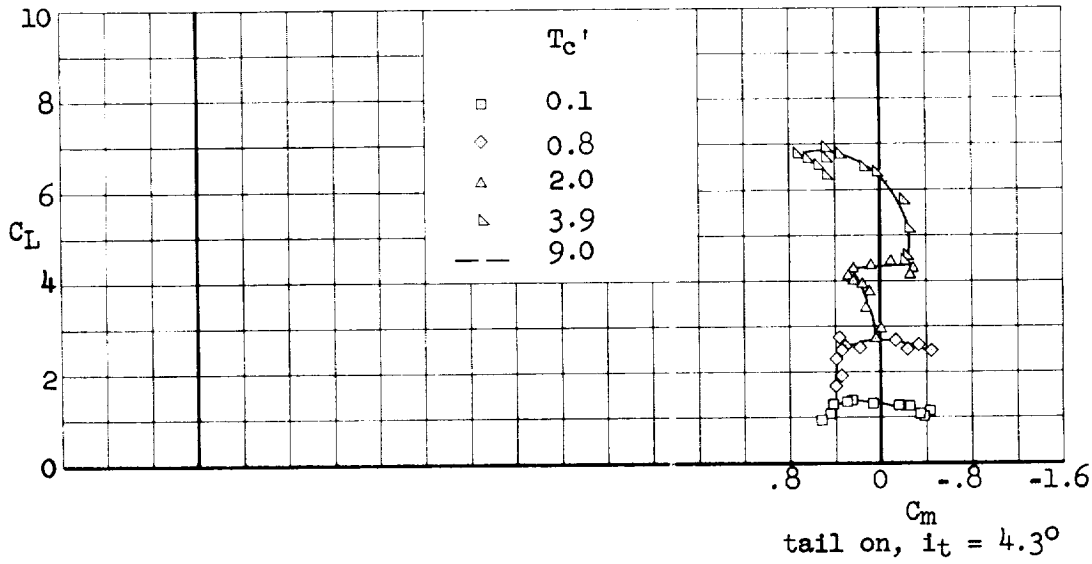

(b) $\delta_f = 50°$, $C_\mu = 0$

Figure 5.- Continued.

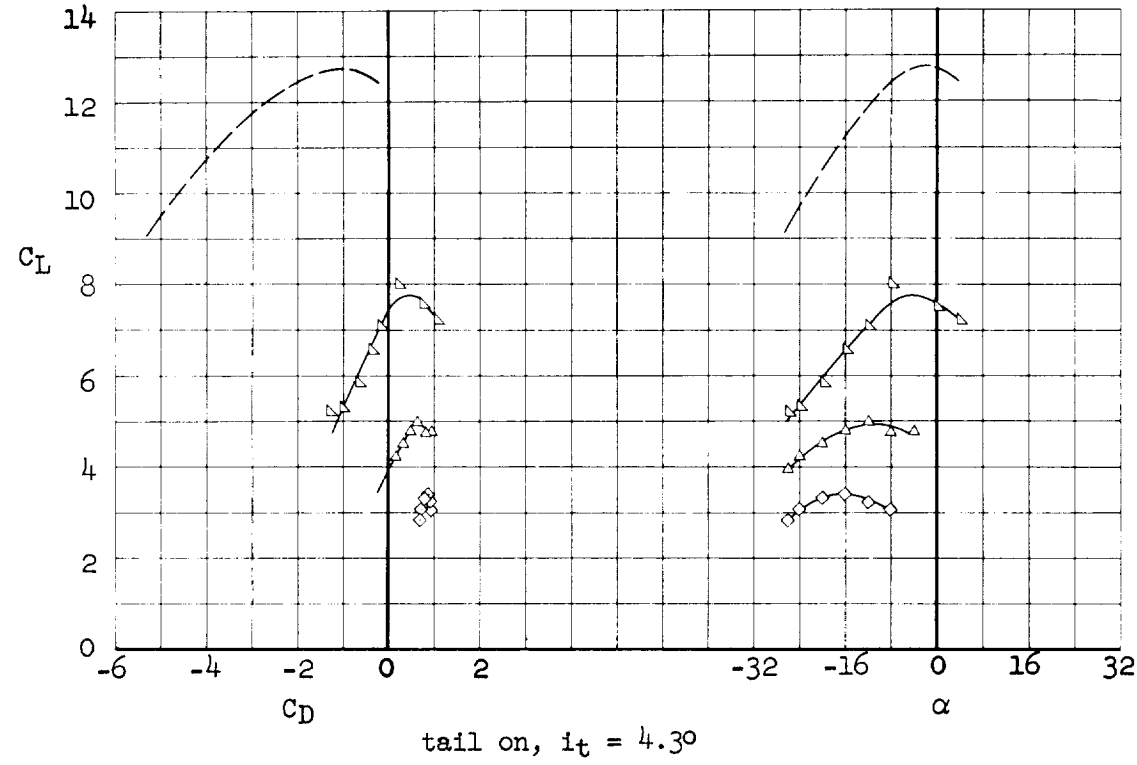

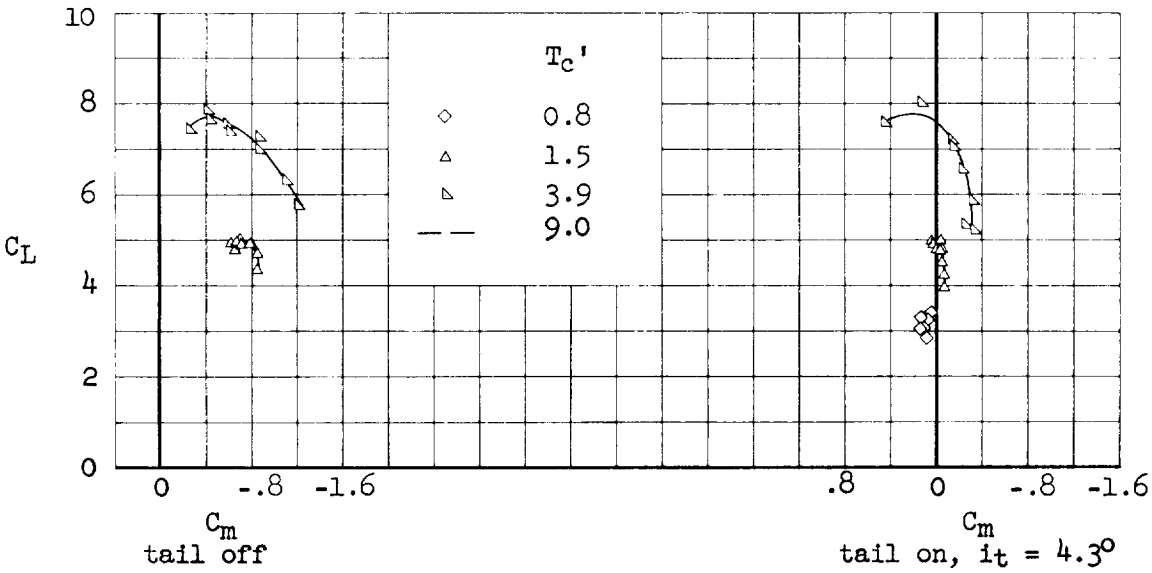

(c) $\delta_f = 50°$, $C_\mu = 0.065$

Figure 5.- Continued.

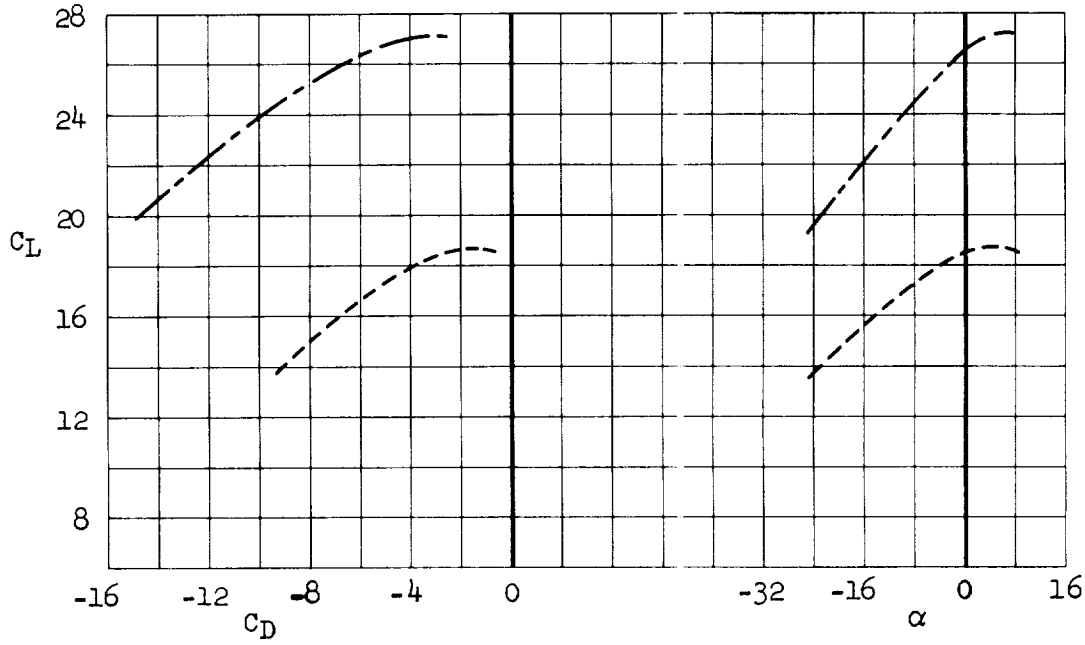

(d) $\delta_f = 50°$, $C_\mu = 0.065$, $i_t = 4.3°$

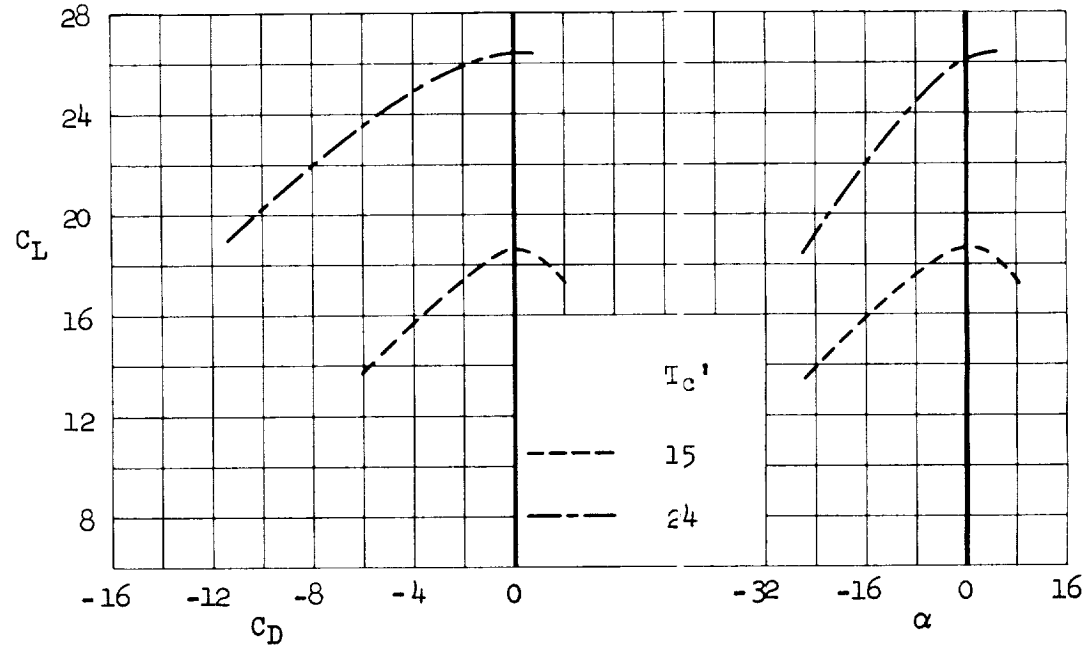

(e) $\delta_f = 80°$, $C_\mu = 0.092$, $i_t = 4.3°$

Figure 5.- Continued.

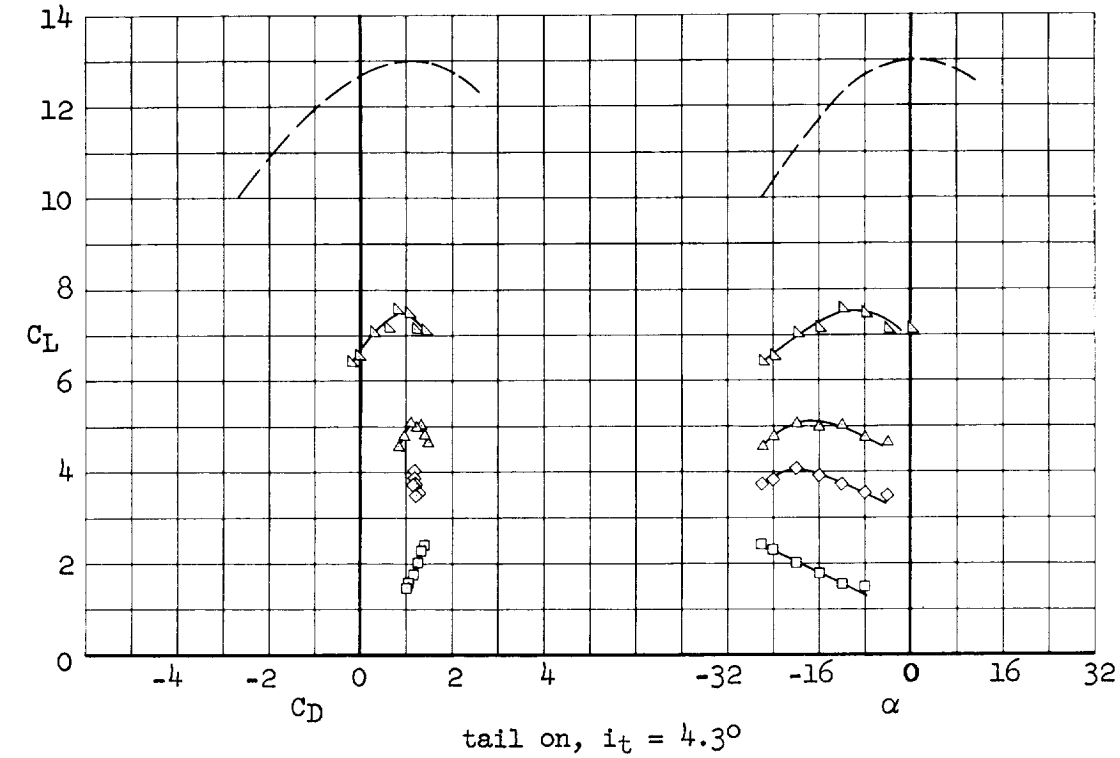

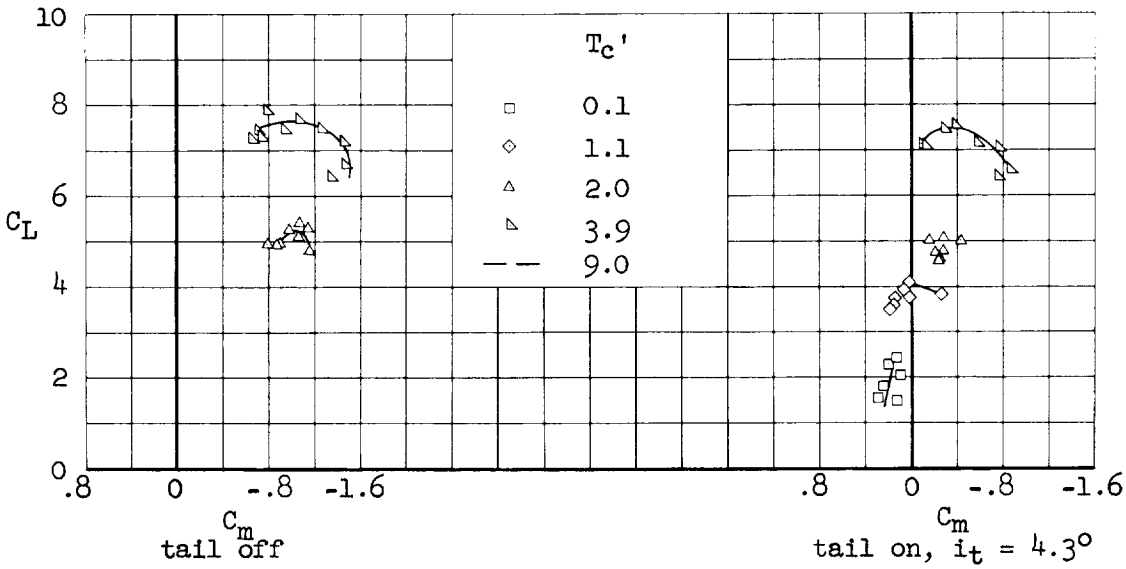

(f) δ_f = 80°, C_μ = 0.092

Figure 5.- Concluded.

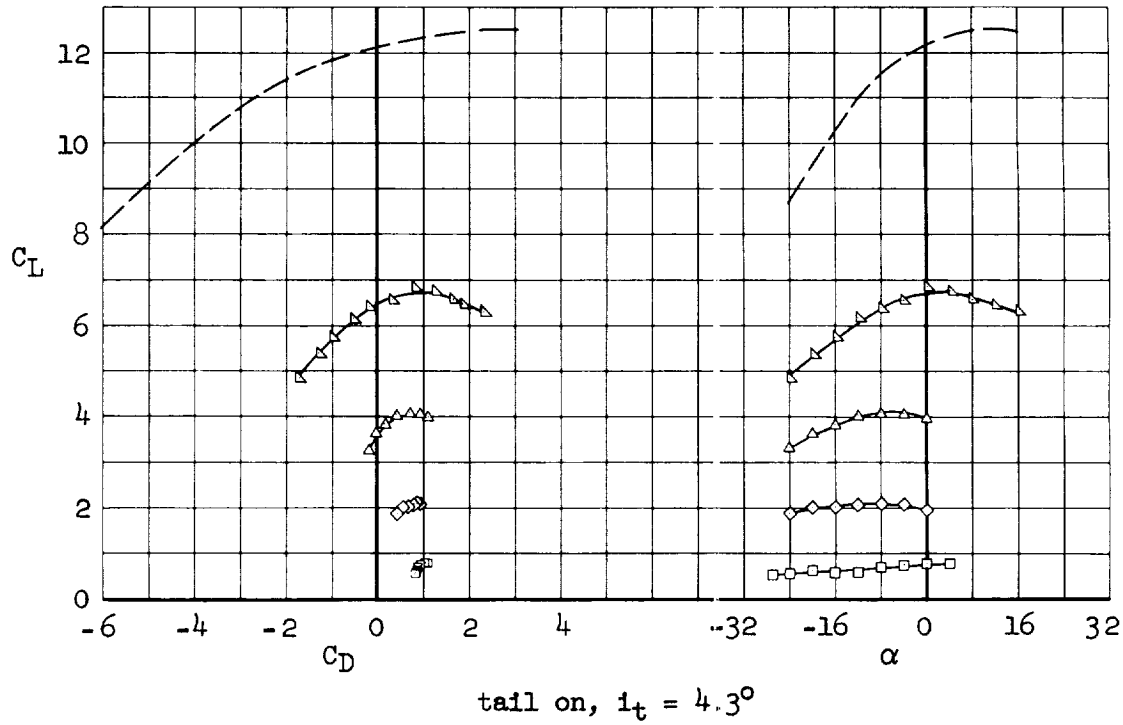

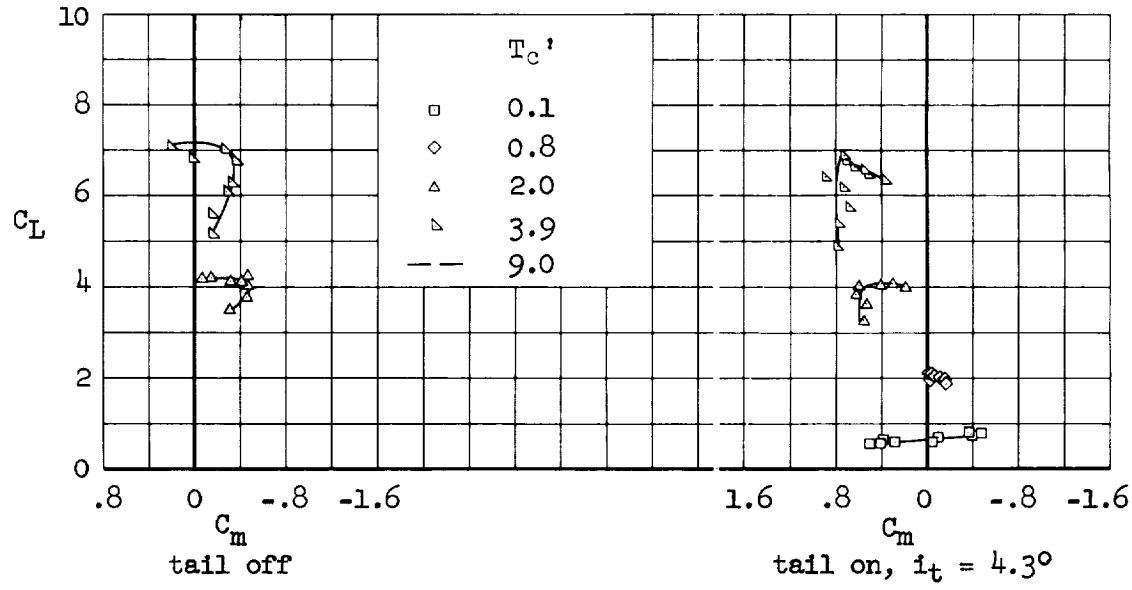

(a) δ_f = 0°, C_μ = (

Figure 6.- Aerodynamic characteristics of the model with 50° wing tilt.

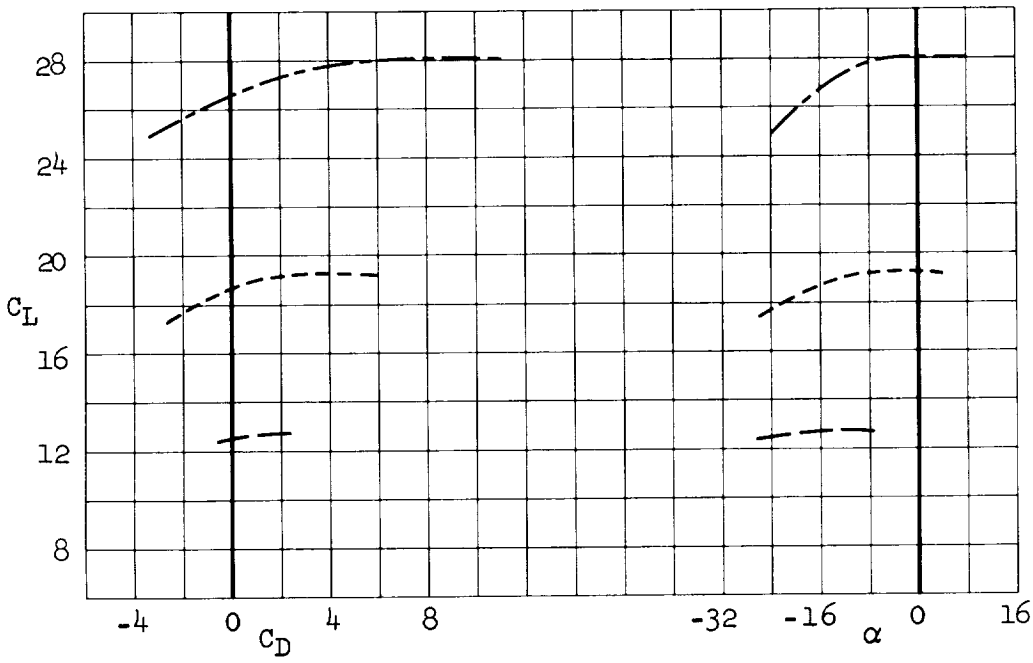

(b) $\delta_f = 50°$, $C_\mu = 0.065$, $i_t = 14°$

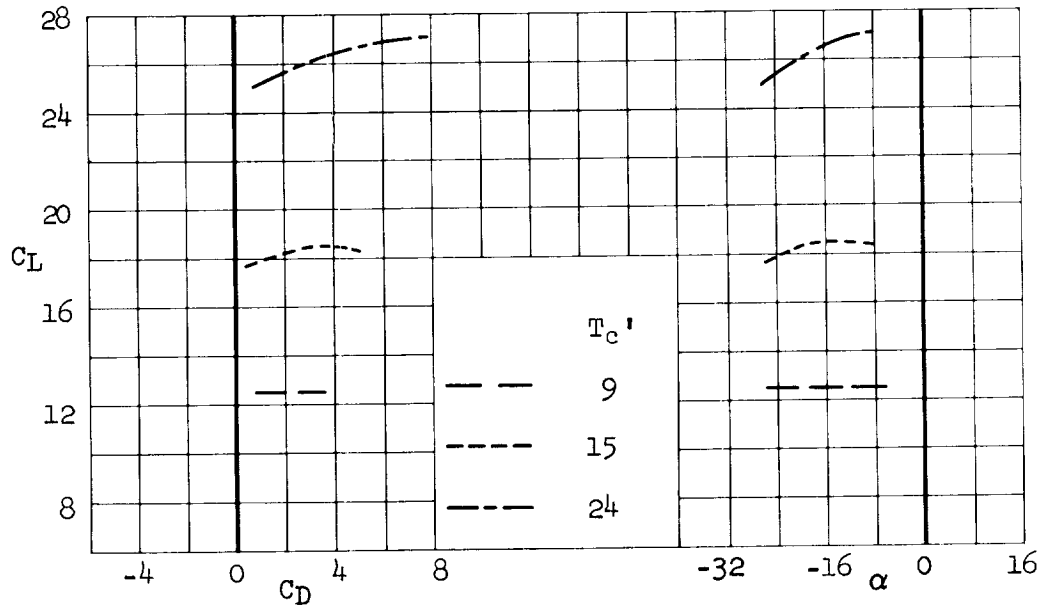

(c) $\delta_f = 80°$, $C_\mu = 0.092$, $i_t = 14°$

Figure 6.- Concluded.

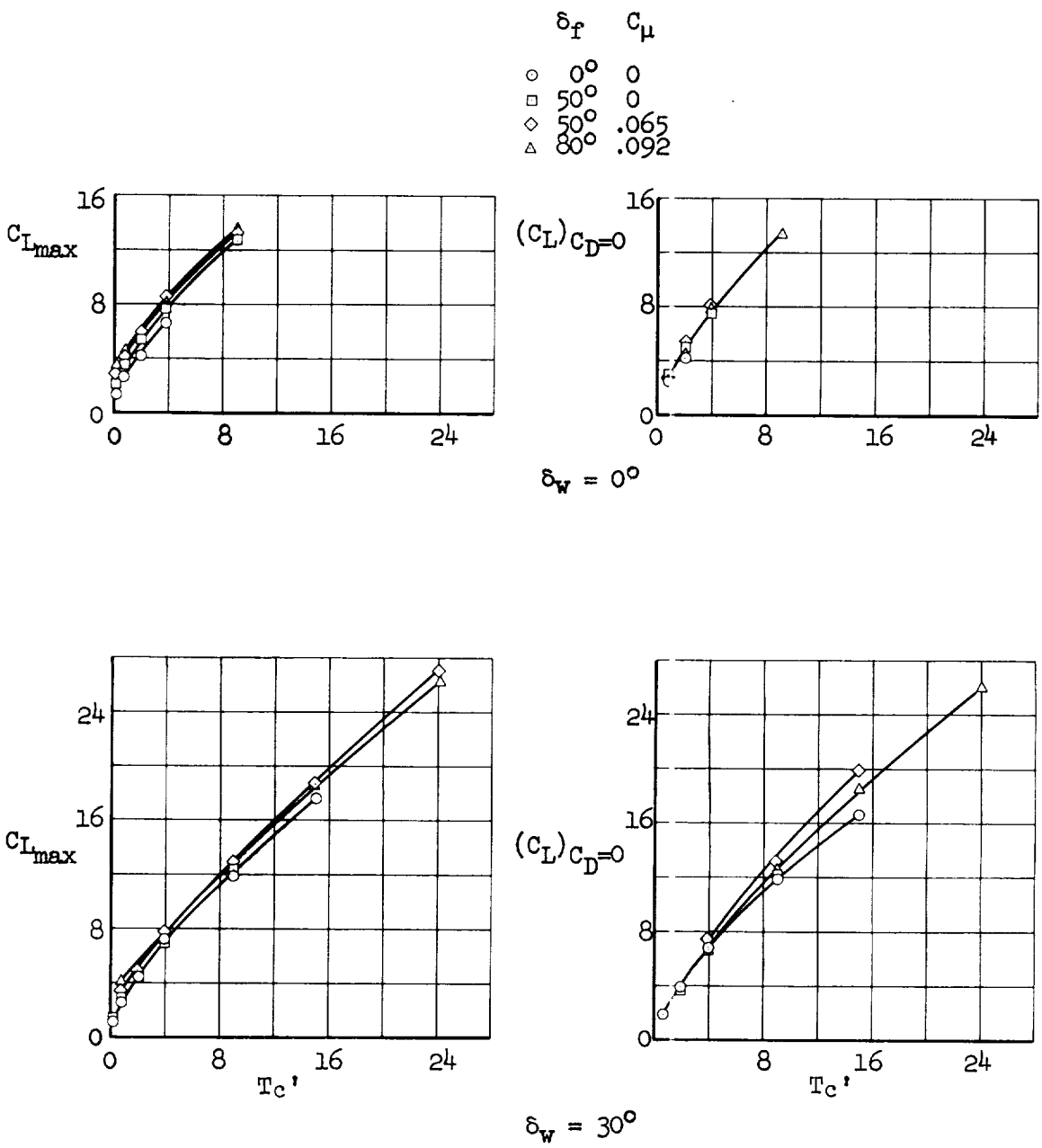

(a) Variation with thrust coefficient of $C_{L_{max}}$ and C_L for level flight (C_D = 0); i_t = 4.3°.

Figure 7.- Summary of lift characteristics.

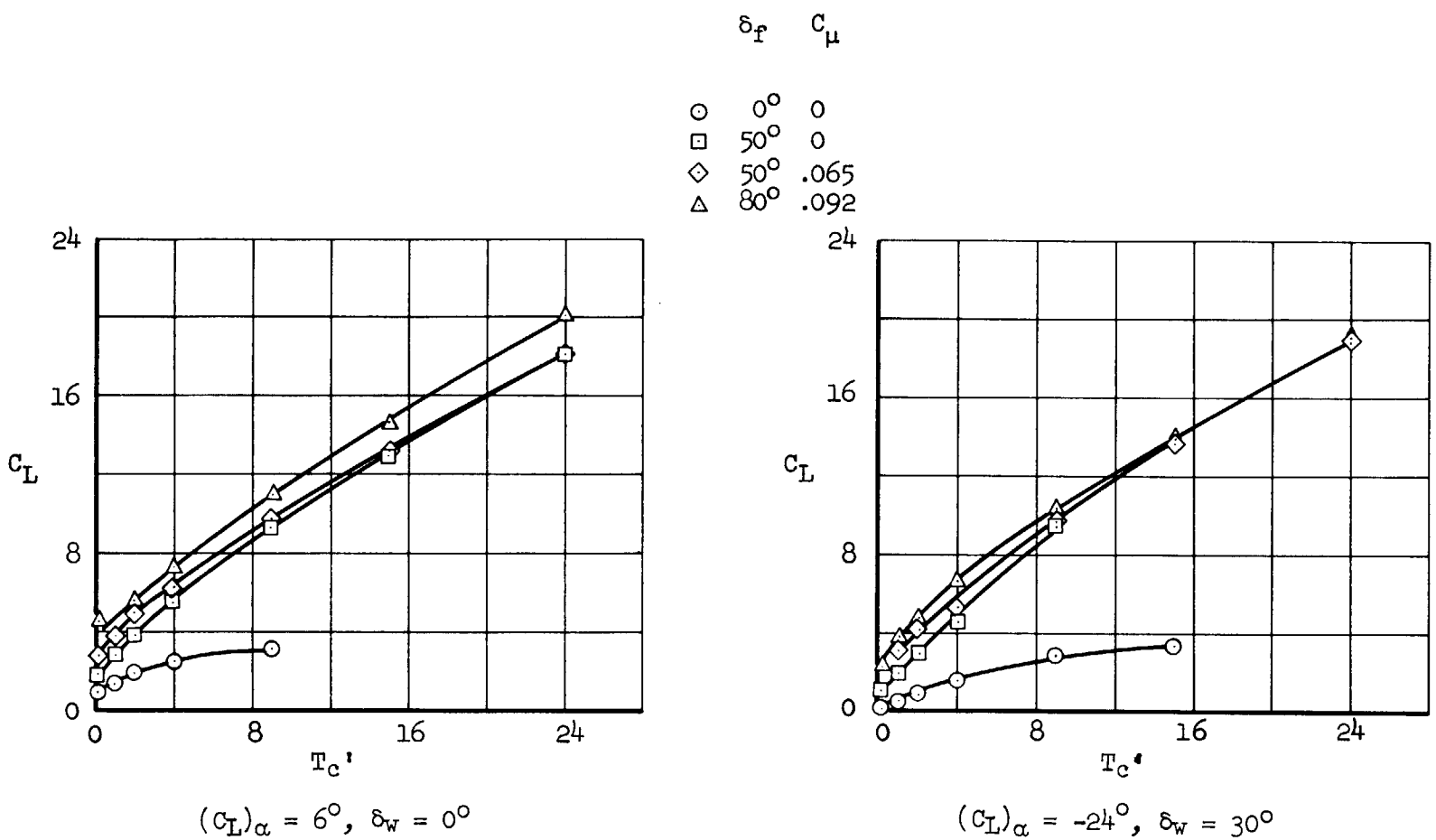

(b) Variation of lift with thrust coefficient at constant angle of attack; $i_t = 4.3°$.

Figure 7.- Continued.

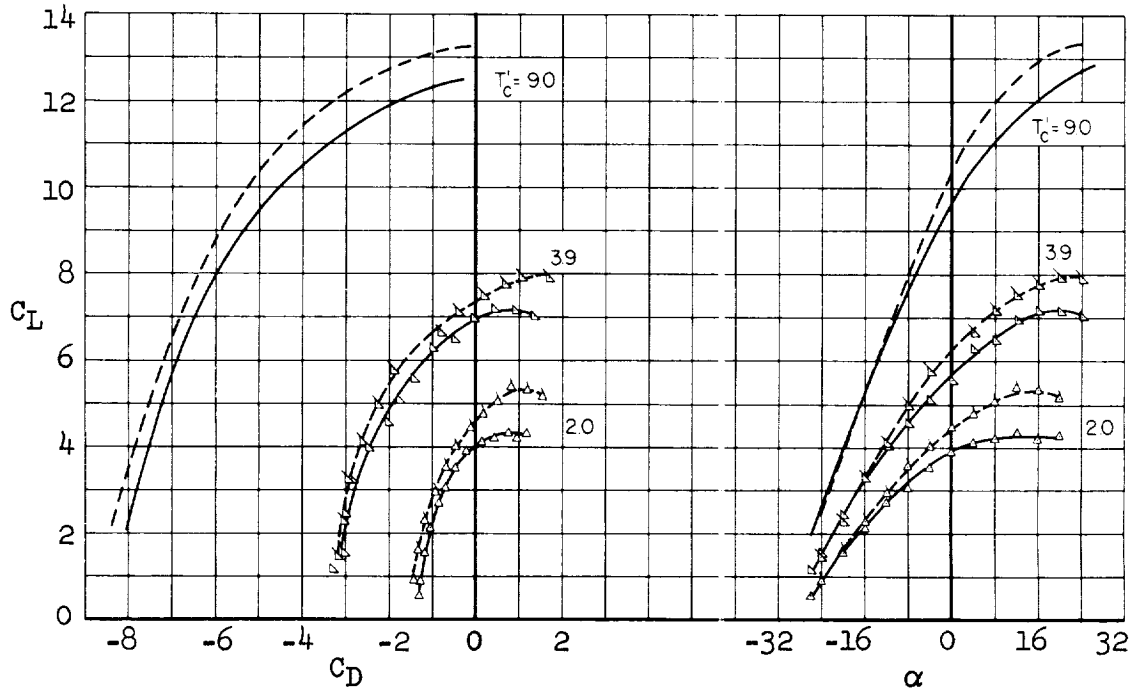

(a) $\delta_f = 0^\circ$, $C_\mu = 0$

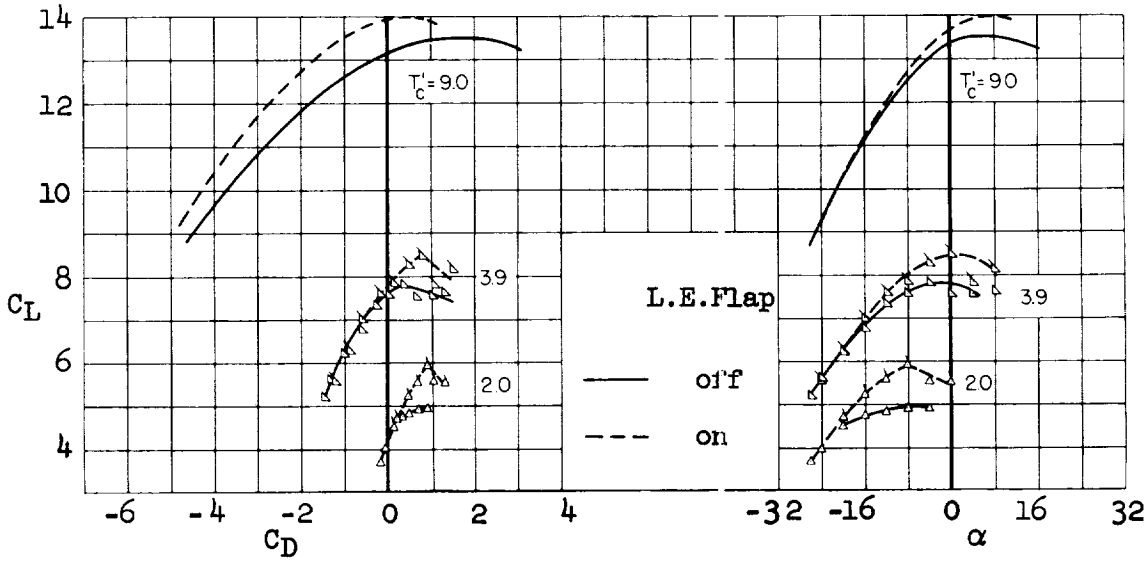

(b) $\delta_f = 50^\circ$, $C_\mu = 0.065$

Figure 9.- Effect of a leading-edge flap on the aerodynamic characteristics of the model with 30° wing tilt; $i_t = 14^\circ$.

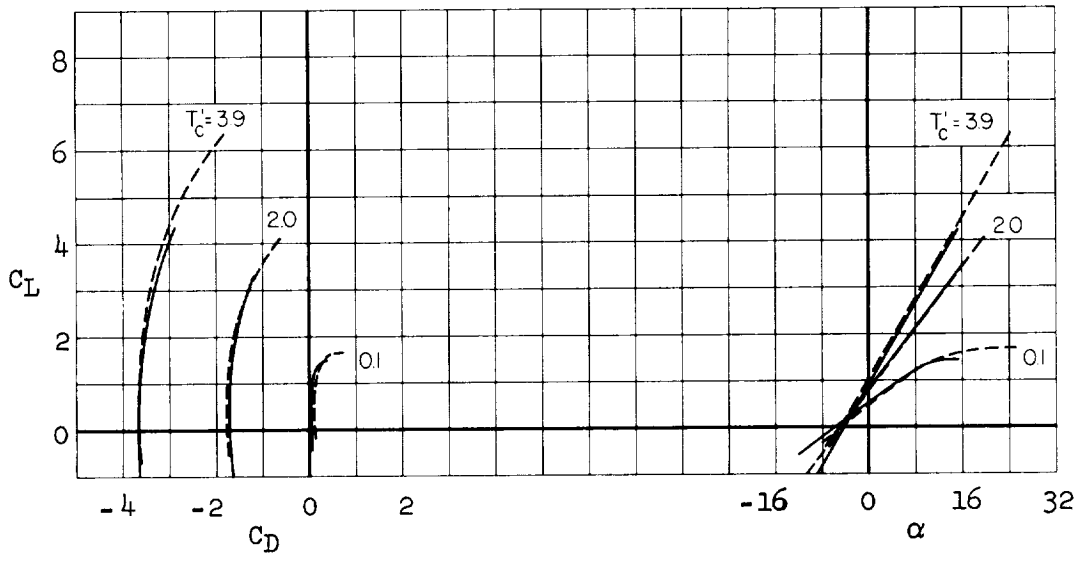

tail on, $i_t = 4.3^\circ$

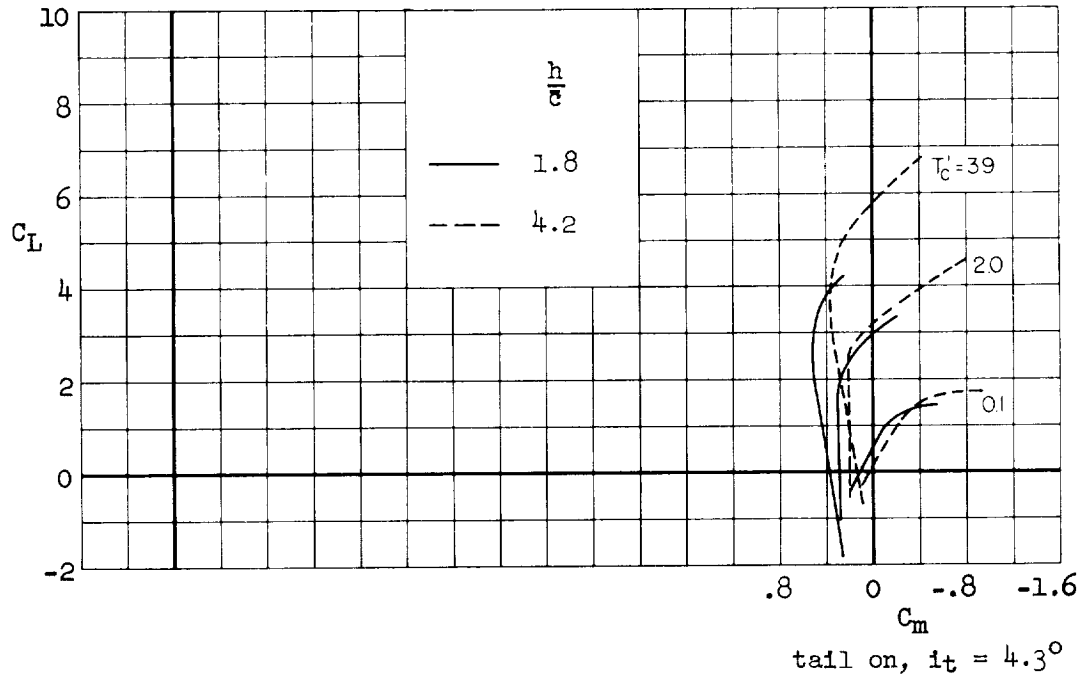

tail on, $i_t = 4.3^\circ$

(a) $\delta_f = 0^\circ$, $C_\mu = 0$

Figure 10.- Effect of ground height on the aerodynamic characteristics of the model.

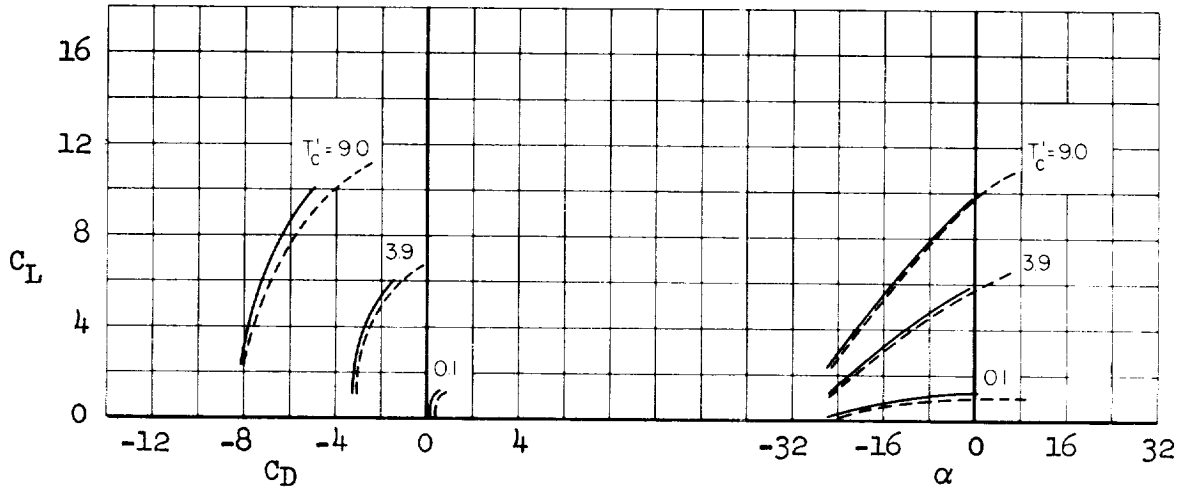

(b) $\delta_f = 0°$, $\delta_w = 30°$, $C_\mu = 0$, $i_t = 4.3°$

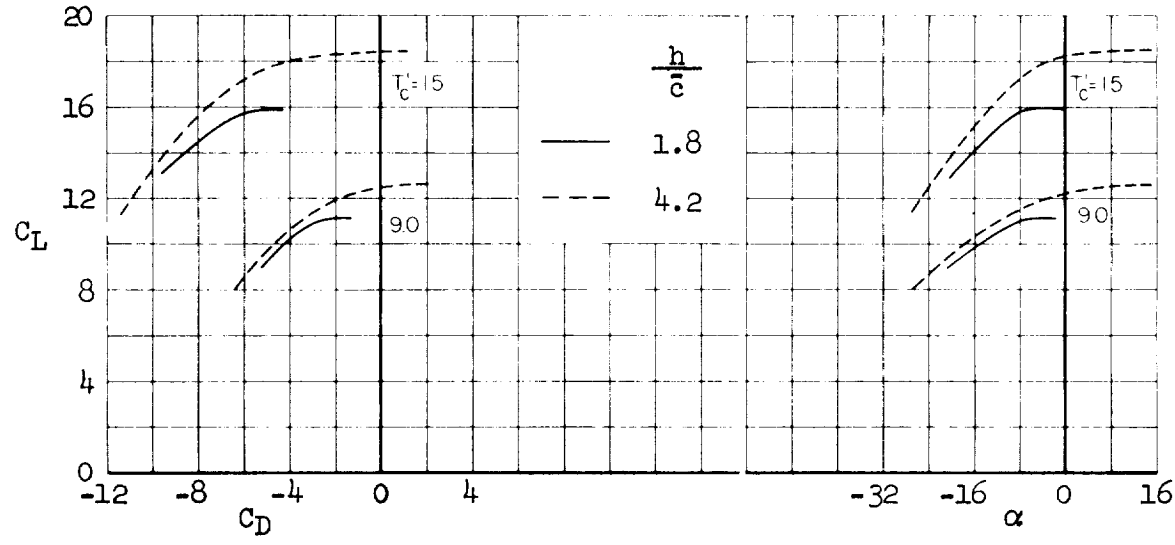

(c) $\delta_f = 0°$, $\delta_w = 50°$, $C_\mu = 0$, $i_t = 4.3°$

Figure 10.- Continued.

A
5
2
4

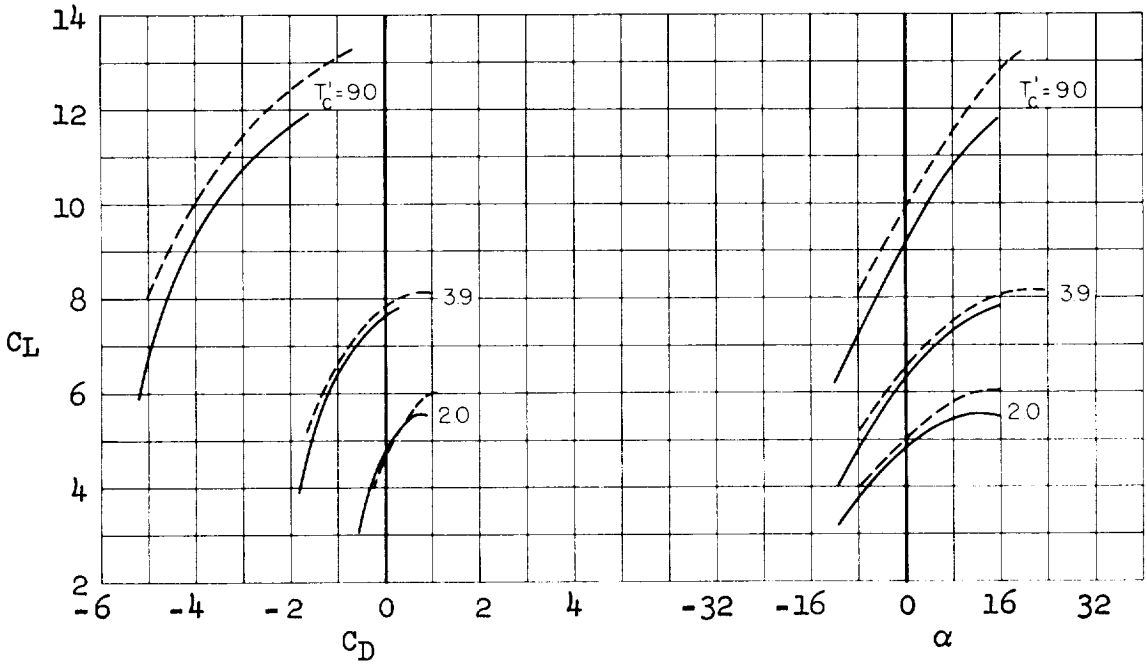

tail on, $i_t = 4.3^\circ$

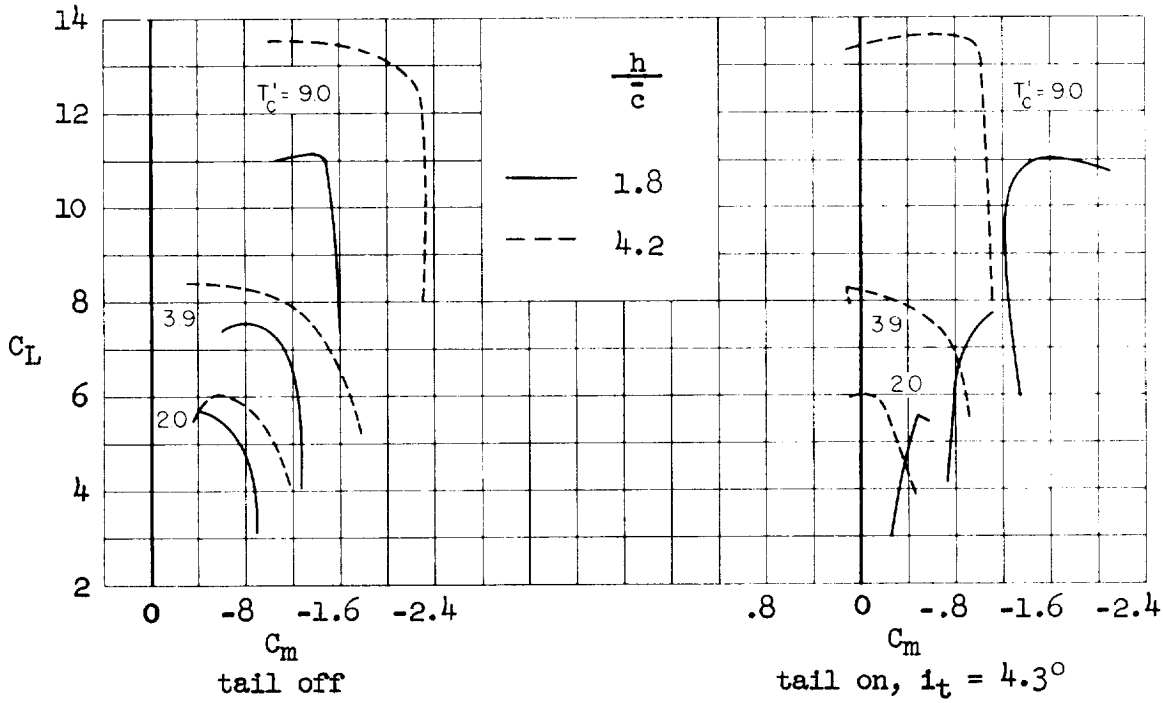

(d) $\delta_f = 80^\circ$, $\delta_w = 0^\circ$, $C_\mu = 0.092$

Figure 10.- Continued.

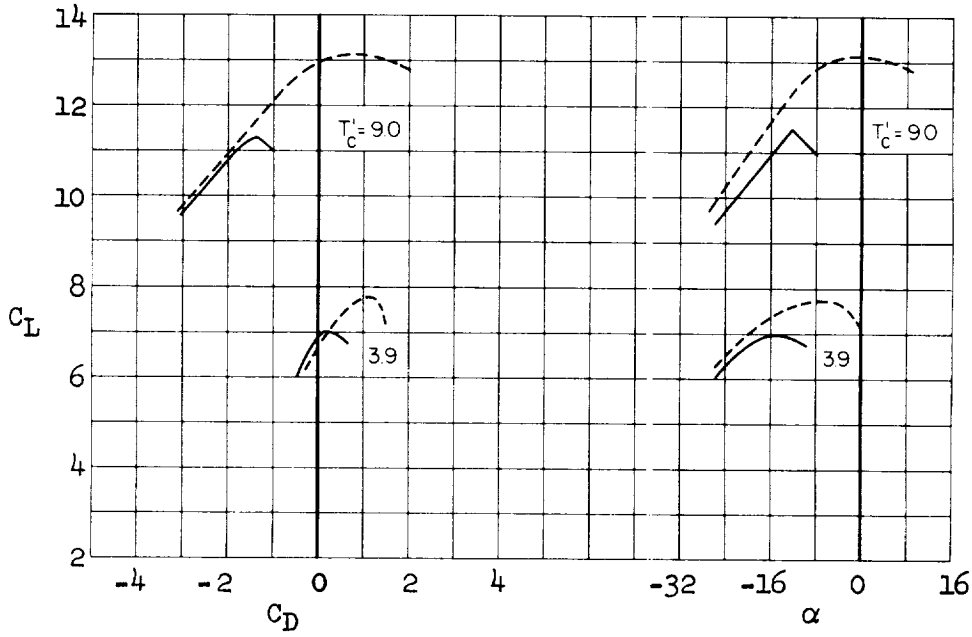

tail on, $i_t = 14^\circ$

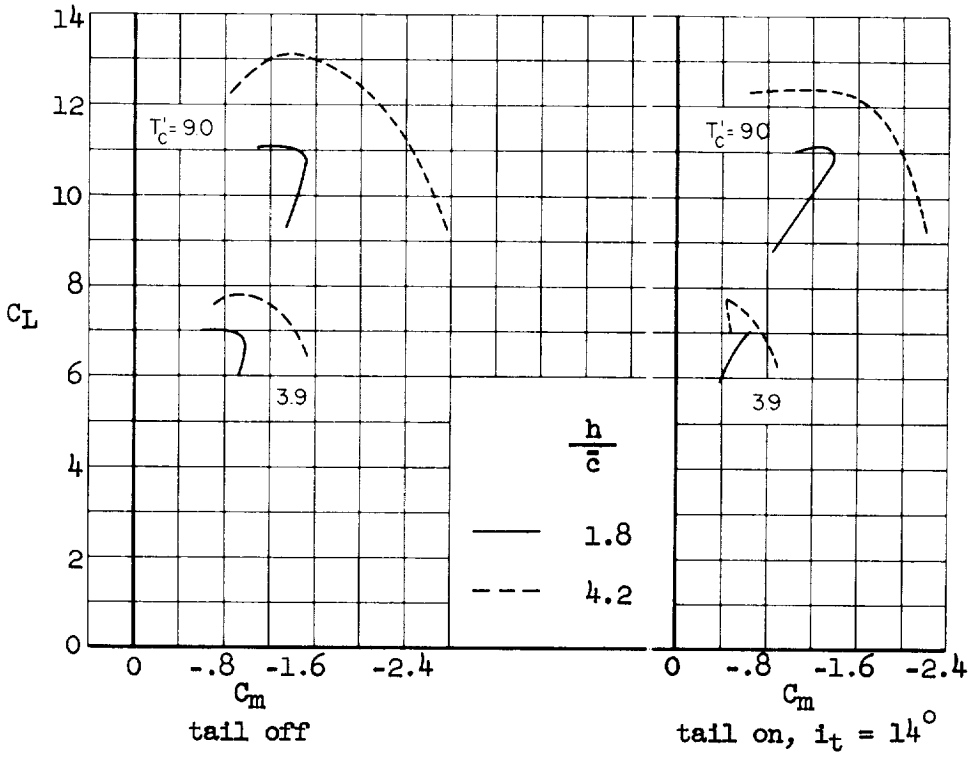

(e) $\delta_f = 80^\circ$, $\delta_w = 30^\circ$, $C_\mu = 0.092$

Figure 10.- Concluded.

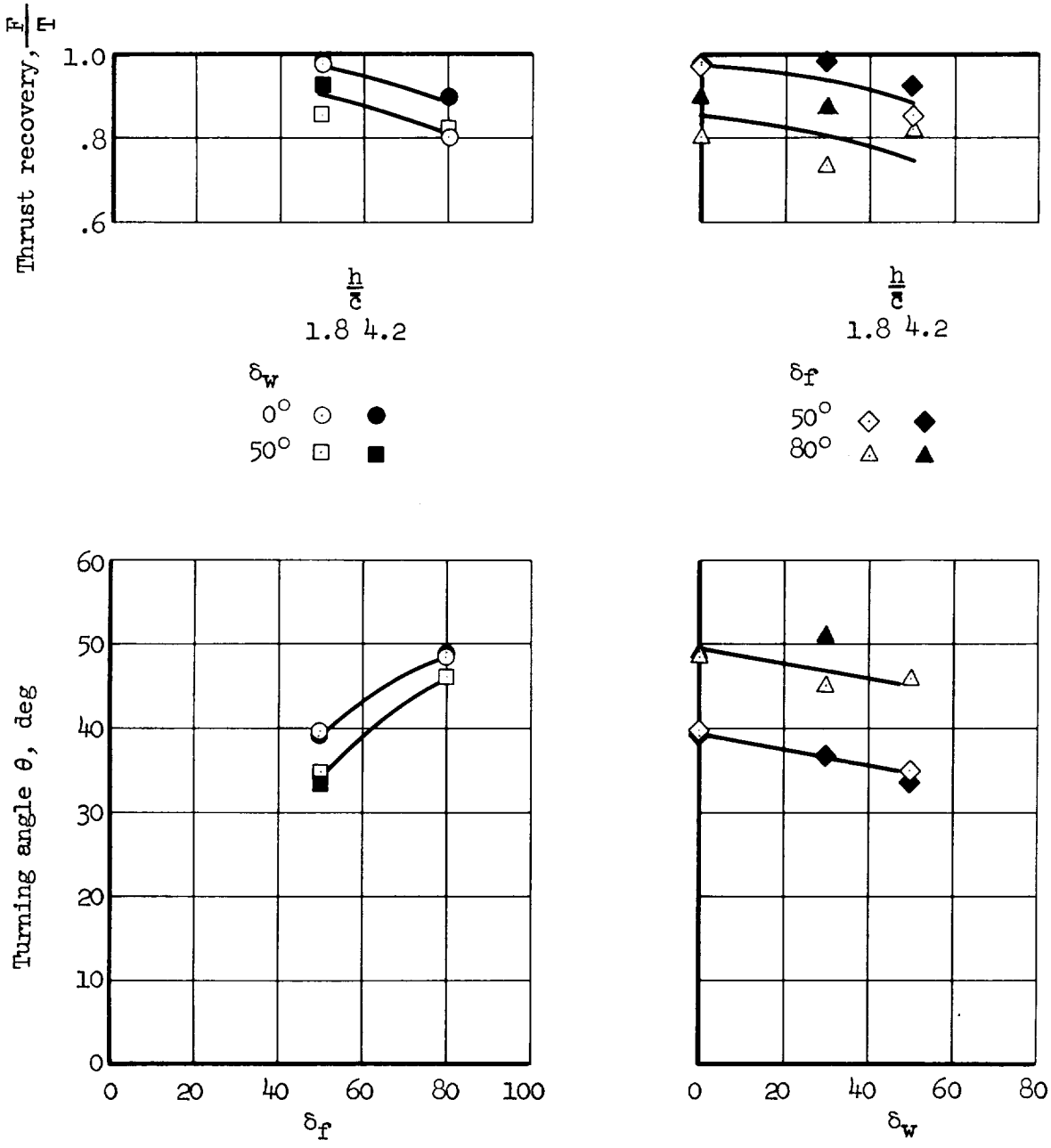

Figure 11.- Effect of ground height on the static hover characteristics; BLC on.